




NSF Engineering Research Center for
Computer Integrated Surgical Systems and
Technology



LABORATORY FOR
**Computational
Sensing + Robotics**
THE JOHNS HOPKINS UNIVERSITY

Registration – Part 2

600.455/655 Computer Integrated Surgery




100 YEARS
JOHNS HOPKINS ENGINEERING

**WHITING
SCHOOL OF
ENGINEERING**
THE JOHNS HOPKINS UNIVERSITY

Russell H. Taylor

John C. Malone Professor of Computer Science,
with joint appointments in Mechanical Engineering, Radiology & Surgery
Director, Laboratory for Computational Sensing and Robotics
The Johns Hopkins University
rht@jhu.edu



1

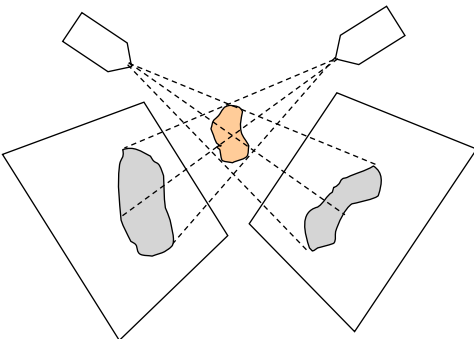
Feature-Based 2D-3D Registration

Given

- 3D surface model of an anatomic structure
- Multiple 2D x-ray projection images taken at known poses relative to some coordinate system C
- Initial estimate of the pose F of the anatomic object relative to the x-ray imaging coordinate system C


Goal

- Compute an accurate value for F

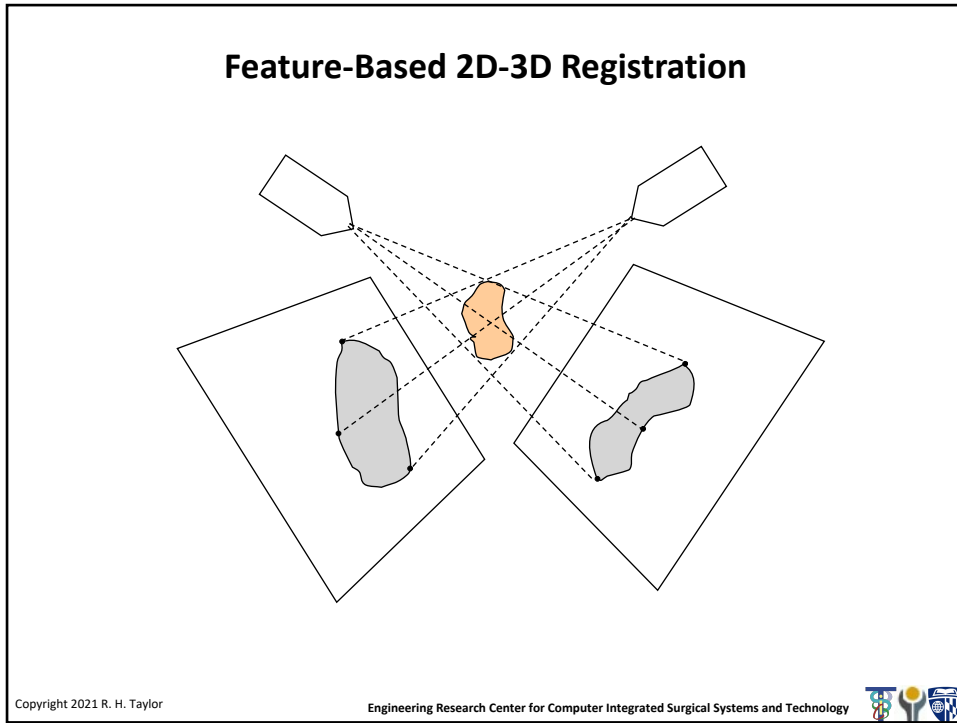


Copyright 2021 R. H. Taylor

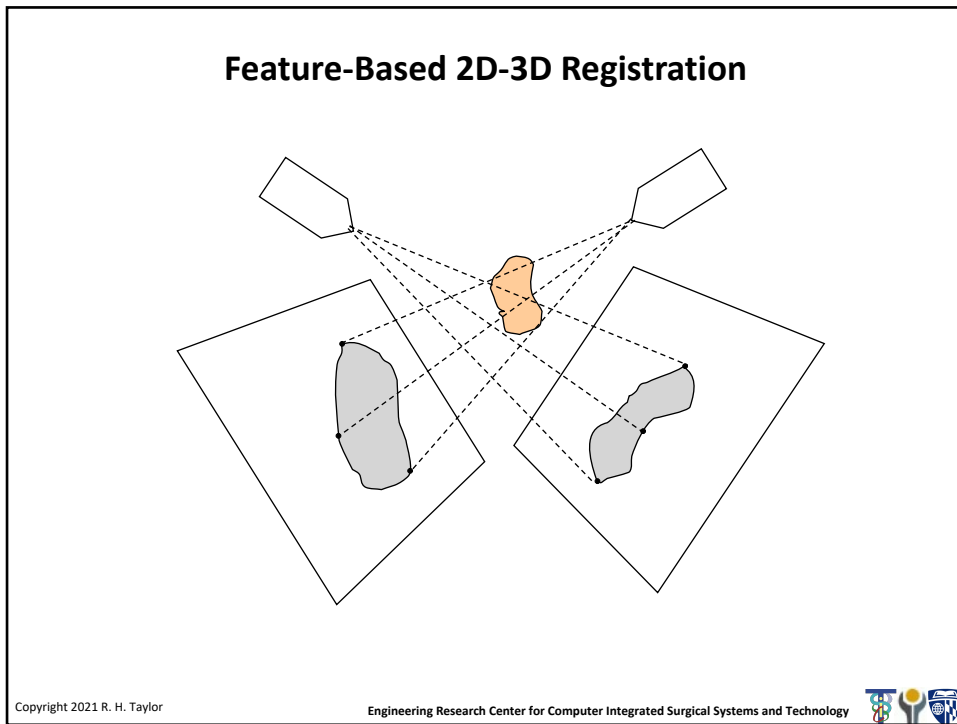
Engineering Research Center for Computer Integrated Surgical Systems and Technology



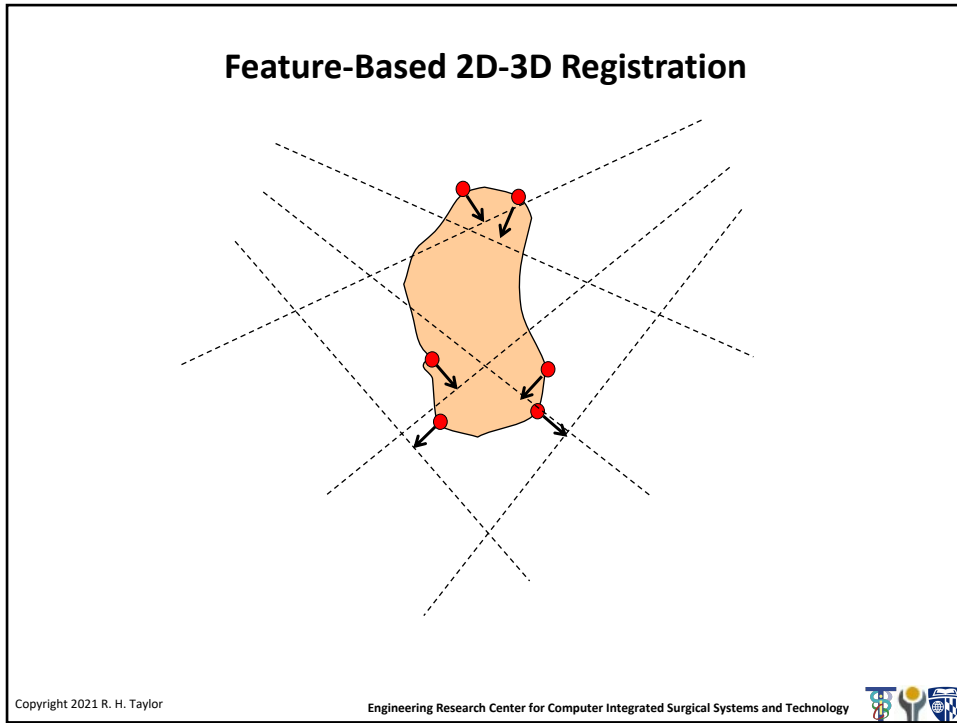
2



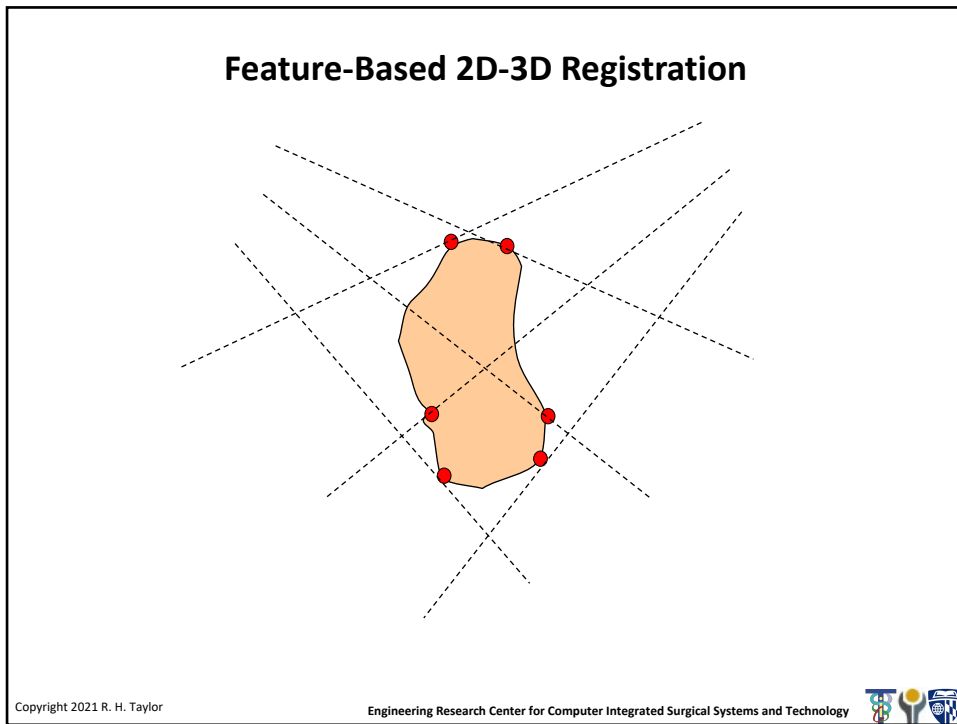
3



4



5



6

Feature-Based 2D-3D Registration

Copyright 2021 R. H. Taylor

Engineering Research Center for Computer Integrated Surgical Systems and Technology

7

A contour-based 2D-3D method ...

Guezic et al., 1998

Step 0: Extract contours from x-ray images and compute corresponding lines between source and detector

A. Guéziec, P. Kazanzides, B. Williamson, and R. Taylor, "Anatomy-Based Registration of CT-Scan and Intraoperative X-Ray Images for Guiding a Surgical Robot," IEEE Transactions on Medical Imaging, vol. 17, pp. 715-728, 1998.

Copyright 2021 R. H. Taylor

Engineering Research Center for Computer Integrated Surgical Systems and Technology

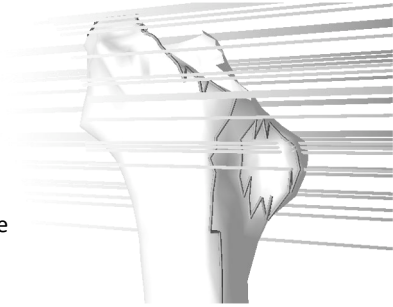
8

A contour-based 2D-3D method ...

Guezic et al., 1998

Step 1: Given the current estimate for $F = [R,t]$, compute the apparent projection contours of the model for each viewing direction.

Step 2: For each x-ray path line L_i , identify the closest point p_i on an apparent projection contour. This will give a set of points on the body surface to be moved toward the corresponding x-ray lines



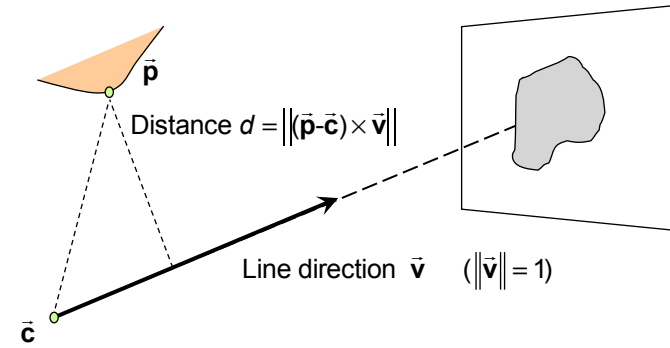
A. Guéziec, P. Kazanzides, B. Williamson, and R. Taylor, "Anatomy-Based Registration of CT-Scan and Intraoperative X-Ray Images for Guiding a Surgical Robot," IEEE Transactions on Medical Imaging, vol. 17, pp. 715-728, 1998.

Copyright 2021 R. H. Taylor Engineering Research Center for Computer Integrated Surgical Systems and Technology

9

A contour-based 2D-3D method ...

Guezic et al., 1998



Distance $d = \|(\vec{p} - \vec{c}) \times \vec{v}\|$

Line direction \vec{v} ($\|\vec{v}\| = 1$)

Note: It is convenient to use the x-ray source position (i.e., the center of convergence for a bundle of x-ray projection lines) as the value for \vec{c} .

A. Guéziec, P. Kazanzides, B. Williamson, and R. Taylor, "Anatomy-Based Registration of CT-Scan and Intraoperative X-Ray Images for Guiding a Surgical Robot," IEEE Transactions on Medical Imaging, vol. 17, pp. 715-728, 1998.

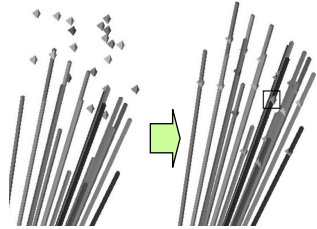
Copyright 2021 R. H. Taylor Engineering Research Center for Computer Integrated Surgical Systems and Technology

10

A contour-based 2D-3D method ...

Guezic et al., 1998

Step 3: Solve an optimization problem to compute a value of F that minimizes the distance between the p_i and the L_i .



$$\min_{\mathbf{R}, \mathbf{t}} \sum_i d_i^2 = \min_{\mathbf{R}, \mathbf{t}} \sum_i \left\| \bar{\mathbf{v}}_i \times (\mathbf{c}_i - (\mathbf{R}\bar{\mathbf{p}}_i + \bar{\mathbf{t}})) \right\|^2$$

$$= \min_{\mathbf{R}, \mathbf{t}} \sum_i \left\| \text{skew}(\bar{\mathbf{v}}_i) \bullet (\mathbf{c}_i - (\mathbf{R}\bar{\mathbf{p}}_i + \bar{\mathbf{t}})) \right\|^2$$

Step 4: Iterate steps 1-3 until reach convergence

A. Guézic, P. Kazanzides, B. Williamson, and R. Taylor, "Anatomy-Based Registration of CT-Scan and Intraoperative X-Ray Images for Guiding a Surgical Robot," IEEE Transactions on Medical Imaging, vol. 17, pp. 715-728, 1998.

Copyright 2021 R. H. Taylor

Engineering Research Center for Computer Integrated Surgical Systems and Technology



11

Computational Note

Guezic uses the Cayley parameterization for rotations:

$$\mathbf{R}(\bar{\mathbf{u}}) = (\mathbf{I} - \text{skew}(\bar{\mathbf{u}}))(\mathbf{I} + \text{skew}(\bar{\mathbf{u}}))^{-1}$$

This leads to the approximation

$$\mathbf{R}(\bar{\mathbf{u}}) \approx \mathbf{I} + \text{skew}(2\bar{\mathbf{u}})$$

which is similar to our familiar $\mathbf{R}(\bar{\alpha}) \approx \mathbf{I} + \text{skew}(\bar{\alpha})$.

He also uses the notation $\mathbf{U} = \text{skew}(\bar{\mathbf{u}})$. So $\mathbf{R}(\bar{\mathbf{u}}) = (\mathbf{I} - \mathbf{U})(\mathbf{I} + \mathbf{U})^{-1}$

Similarly, we will see $\mathbf{V} = \text{skew}(\bar{\mathbf{v}})$, etc.

Copyright 2021 R. H. Taylor

Engineering Research Center for Computer Integrated Surgical Systems and Technology



12

A contour-based 2D-3D method ...

Guezic et al., 1998

Guezic compared three different methods for performing the minimization in Step 3:

- Levenberg Marquardt (LM) nonlinear minimization.
- Linearization and constrained minimization
- Use of a Robust M-Estimator

A. Guéziec, P. Kazanzides, B. Williamson, and R. Taylor, "Anatomy-Based Registration of CT-Scan and Intraoperative X-Ray Images for Guiding a Surgical Robot," IEEE Transactions on Medical Imaging, vol. 17, pp. 715-728, 1998.

Copyright 2021 R. H. Taylor

Engineering Research Center for Computer Integrated Surgical Systems and Technology



13

Levenberg-Marquardt ...

(Following development in Guezic et al., 1998)

Define $f_i(\vec{x}) = \|\mathbf{V}_i(\vec{\mathbf{c}}_i - \mathbf{R}(\vec{\mathbf{u}})\vec{\mathbf{p}}_i - \vec{\mathbf{t}})\|$ where $\vec{x}^t = [\vec{\mathbf{u}}^t, \vec{\mathbf{t}}^t]$, $\mathbf{V}_i = \text{skew}(\vec{\mathbf{v}}_i)$

Our goal is to minimize

$$\varepsilon(\vec{x}) = \sum_i f_i(\vec{x})^2 = \sum_i \|\mathbf{V}_i(\vec{\mathbf{c}}_i - \mathbf{R}(\vec{\mathbf{u}})\vec{\mathbf{p}}_i - \vec{\mathbf{t}})\|^2$$

We note that $\varepsilon(\vec{x})$ is nonlinear. Levenberg-Marquardt is a widely used optimization method for problems of this type. However, it requires us to evaluate the partial derivatives $\partial f_i / \partial x_j$. Guezic worked these out symbolically for his problem

A. Guéziec, P. Kazanzides, B. Williamson, and R. Taylor, "Anatomy-Based Registration of CT-Scan and Intraoperative X-Ray Images for Guiding a Surgical Robot," IEEE Transactions on Medical Imaging, vol. 17, pp. 715-728, 1998.

Copyright 2021 R. H. Taylor

Engineering Research Center for Computer Integrated Surgical Systems and Technology



14

Levenberg-Marquardt ...

(Following development in Guezic et al., 1998)

Define $f_i(\vec{x}) = \|\mathbf{V}_i(\vec{c}_i - \mathbf{R}(\vec{u})\vec{p}_i - \vec{t})\|$ where $\vec{x}^t = [\vec{u}^t, \vec{t}^t]$, $\mathbf{V}_i = \text{skew}(\vec{v}_i)$

$$\mathbf{J} = \begin{bmatrix} \dots & \frac{\partial f_i}{\partial \vec{x}} & \dots \end{bmatrix} = \begin{bmatrix} \dots & \frac{\partial f_i}{\partial \vec{u}} & \dots \\ \dots & \frac{\partial f_i}{\partial \vec{t}} & \dots \end{bmatrix}$$

$$\frac{\partial f_i}{\partial \vec{t}} = \frac{\mathbf{V}_i^t \mathbf{V}_i (\mathbf{R}\vec{p}_i - \mathbf{c} + \vec{t})}{f_i}$$

$$\frac{\partial f_i}{\partial \vec{u}} = \left(\frac{\partial \mathbf{R}\vec{p}_i}{\partial \vec{u}} \right)^t \frac{\mathbf{V}_i^t \mathbf{V}_i (\mathbf{R}\vec{p}_i - \mathbf{c} + \vec{t})}{f_i}$$

Details on this may be found
in reference [45] of
Guezic's paper

A. Guéziec, P. Kazanzides, B. Williamson, and R. Taylor, "Anatomy-Based Registration of CT-Scan and Intraoperative X-Ray Images for Guiding a Surgical Robot," IEEE Transactions on Medical Imaging, vol. 17, pp. 715-728, 1998.

Copyright 2021 R. H. Taylor

Engineering Research Center for Computer Integrated Surgical Systems and Technology



15

Levenberg-Marquardt ...

(Following development in Guezic et al., 1998)

Step 1: Pick $\lambda =$ a small number; pick initial guess for \vec{x}

Step 2: Evaluate $f_i(\vec{x})$ and \mathbf{J} and solve the least squares problem

$$\begin{bmatrix} \vdots \\ (\mathbf{J}^t \mathbf{J} + \lambda \mathbf{I}) \Delta \vec{x} - \mathbf{J}^t f_i \\ \vdots \end{bmatrix} = \begin{bmatrix} \vdots \\ 0 \\ \vdots \end{bmatrix}$$

for $\Delta \vec{x}$.

Step 3: $\vec{x} \leftarrow \vec{x} + \Delta \vec{x}$; update λ .

Step 4: Evaluate termination condition. If not done, go back to step 2

Note: Usually λ starts small and grows larger. Consult standard references (e.g., Numerical Recipes) for more information.

A. Guéziec, P. Kazanzides, B. Williamson, and R. Taylor, "Anatomy-Based Registration of CT-Scan and Intraoperative X-Ray Images for Guiding a Surgical Robot," IEEE Transactions on Medical Imaging, vol. 17, pp. 715-728, 1998.

Copyright 2021 R. H. Taylor

Engineering Research Center for Computer Integrated Surgical Systems and Technology



16

Constrained Linearized Least Squares ...

(Following development in Guezic et al., 1998)

Step 0: Make an initial guess for \mathbf{R} and $\bar{\mathbf{t}}$

Step 1: Compute $\bar{\mathbf{p}}_i \leftarrow \mathbf{R}\mathbf{p}_i + \bar{\mathbf{t}}$

Step 2: Define $\mathbf{P}_i = \text{skew}(\bar{\mathbf{p}}_i)$, $\mathbf{V}_i = \text{skew}(\bar{\mathbf{v}}_i)$

Step 3: Solve the least squares problem:

$$\varepsilon^2 = \min \left\| \begin{bmatrix} \vdots & \vdots \\ 2\mathbf{V}\mathbf{P}_i & \mathbf{V}_i \\ \vdots & \vdots \end{bmatrix} \begin{bmatrix} \bar{\mathbf{u}} \\ \Delta\bar{\mathbf{t}} \end{bmatrix} - \begin{bmatrix} \vdots \\ \mathbf{V}_i(\bar{\mathbf{c}}_i - \bar{\mathbf{p}}_i) \\ \vdots \end{bmatrix} \right\|^2 \quad \text{subject to } \|\bar{\mathbf{u}}\| \leq \rho$$

where ρ is sufficiently small so that $\mathbf{I} + 2\mathbf{U}$ approximates a rotation

Step 4: Compute $\Delta\mathbf{R} = (\mathbf{I} - \mathbf{U})(\mathbf{I} + \mathbf{U})^{-1}$

Update $\mathbf{p}_i \leftarrow \Delta\mathbf{R}\mathbf{p}_i + \Delta\bar{\mathbf{t}}$; $\mathbf{R} \leftarrow \Delta\mathbf{R}\mathbf{R}$; $\bar{\mathbf{t}} \leftarrow \Delta\mathbf{R}\bar{\mathbf{t}} + \Delta\bar{\mathbf{t}}$

Step 5: If ε is small enough or some other termination condition is met, then stop. Otherwise go back to Step 2.

A. Guéziec, P. Kazanzides, B. Williamson, and R. Taylor, "Anatomy-Based Registration of CT-Scan and Intraoperative X-Ray Images for Guiding a Surgical Robot," IEEE Transactions on Medical Imaging, vol. 17, pp. 715-728, 1998.

Copyright 2021 R. H. Taylor

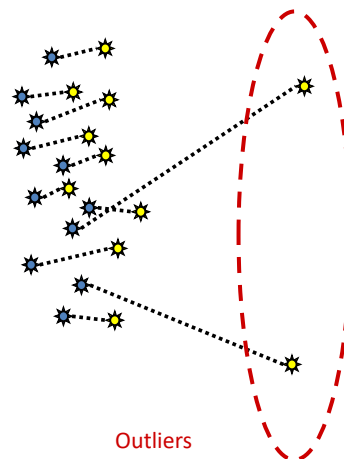
Engineering Research Center for Computer Integrated Surgical Systems and Technology



17

Robust Pose Estimation ...

- Basic idea is to identify outliers and give them little or no weight.



R. Kumar and A. R. Hanson, "Robust methods for estimating pose and a sensitivity analysis," Comput. Vision, Graphics, Image Processing-IV, vol. 60, no. 3, pp. 313-342, 1994.

Copyright 2021 R. H. Taylor

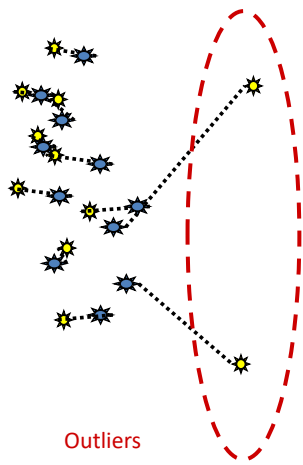
Engineering Research Center for Computer Integrated Surgical Systems and Technology



18

Robust Pose Estimation ...

- Basic idea is to identify outliers and give them little or no weight.



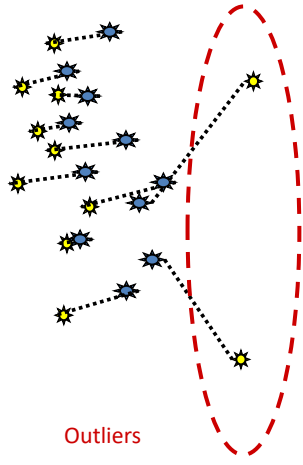
Outliers

R. Kumar and A. R. Hanson, "Robust methods for estimating pose and a sensitivity analysis," *Comput. Vision, Graphics, Image Processing-IU*, vol. 60, no. 3, pp. 313–342, 1994.

Copyright 2021 R. H. Taylor Engineering Research Center for Computer Integrated Surgical Systems and Technology

Robust Pose Estimation ...

- Basic idea is to identify outliers and give them little or no weight.



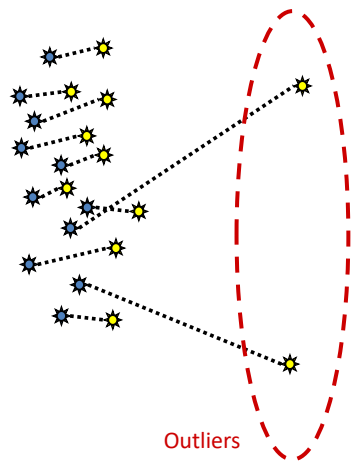
Outliers

R. Kumar and A. R. Hanson, "Robust methods for estimating pose and a sensitivity analysis," *Comput. Vision, Graphics, Image Processing-IU*, vol. 60, no. 3, pp. 313–342, 1994.

Copyright 2021 R. H. Taylor Engineering Research Center for Computer Integrated Surgical Systems and Technology


Robust Pose Estimation ...

- Basic idea is to identify outliers and give them little or no weight.



Outliers

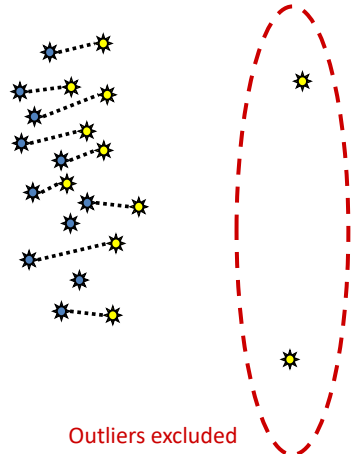
R. Kumar and A. R. Hanson, "Robust methods for estimating pose and a sensitivity analysis," *Comput. Vision, Graphics, Image Processing-IU*, vol. 60, no. 3, pp. 313–342, 1994.

Copyright 2021 R. H. Taylor Engineering Research Center for Computer Integrated Surgical Systems and Technology 

21


Robust Pose Estimation ...

- Basic idea is to identify outliers and give them little or no weight.



Outliers excluded

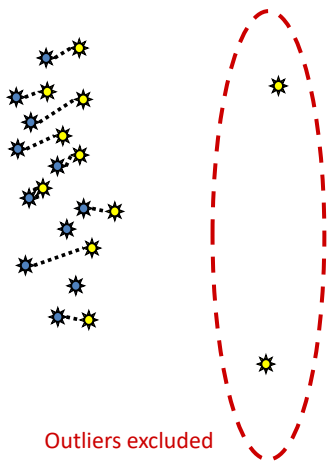
R. Kumar and A. R. Hanson, "Robust methods for estimating pose and a sensitivity analysis," *Comput. Vision, Graphics, Image Processing-IU*, vol. 60, no. 3, pp. 313–342, 1994.

Copyright 2021 R. H. Taylor Engineering Research Center for Computer Integrated Surgical Systems and Technology 

22

Robust Pose Estimation ...

- Basic idea is to identify outliers and give them little or no weight.



Outliers excluded

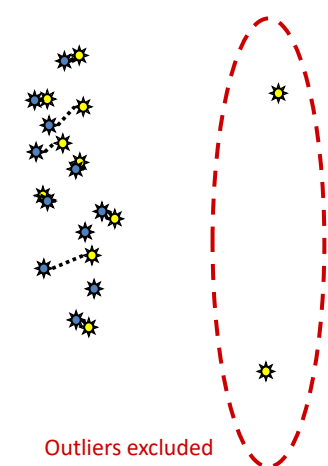
R. Kumar and A. R. Hanson, "Robust methods for estimating pose and a sensitivity analysis," *Comput. Vision, Graphics, Image Processing-IU*, vol. 60, no. 3, pp. 313–342, 1994.

Copyright 2021 R. H. Taylor Engineering Research Center for Computer Integrated Surgical Systems and Technology

23

Robust Pose Estimation ...

- Basic idea is to identify outliers and give them little or no weight.



Outliers excluded

R. Kumar and A. R. Hanson, "Robust methods for estimating pose and a sensitivity analysis," *Comput. Vision, Graphics, Image Processing-IU*, vol. 60, no. 3, pp. 313–342, 1994.

Copyright 2021 R. H. Taylor Engineering Research Center for Computer Integrated Surgical Systems and Technology

24

Robust M-Estimator ...

(Following development in Guezic et al., 1998)

Step 0: Make an initial guess for \mathbf{R} and $\bar{\mathbf{t}}$

Step 1: Compute $\bar{\mathbf{p}}_i \leftarrow \mathbf{R}\bar{\mathbf{p}}_i + \bar{\mathbf{t}}$

Step 2: Define $\mathbf{P}_i = \text{skew}(\bar{\mathbf{p}}_i)$, $\mathbf{V}_i = \text{skew}(\bar{\mathbf{v}}_i)$,

Step 3: Solve a robust linearized problem

$$\varepsilon = \arg \min_{\bar{\mathbf{u}}, \Delta \bar{\mathbf{t}}} \sum_i \rho \left(\frac{0.6745 e_i}{\text{median}(\{e_i\})} \right) \quad \text{where } e_i = \|\mathbf{V}_i(\bar{\mathbf{p}}_i - \mathbf{c}_i + 2\mathbf{P}_i\bar{\mathbf{u}} + \Delta \bar{\mathbf{t}})\|$$

(See next slide)

Step 4: Compute $\Delta \mathbf{R} = (\mathbf{I} - \mathbf{U})(\mathbf{I} + \mathbf{U})^{-1}$

Update $\mathbf{p}_i \leftarrow \Delta \mathbf{R}\mathbf{p}_i + \Delta \bar{\mathbf{t}}$; $\mathbf{R} \leftarrow \Delta \mathbf{R}\mathbf{R}$; $\bar{\mathbf{t}} \leftarrow \Delta \mathbf{R}\bar{\mathbf{t}} + \Delta \bar{\mathbf{t}}$

Step 5: If ε is small enough or some other termination condition is met, then stop. Otherwise go back to Step 2.

A. Guéziec, P. Kazanzides, B. Williamson, and R. Taylor, "Anatomy-Based Registration of CT-Scan and Intraoperative X-Ray Images for Guiding a Surgical Robot," IEEE Transactions on Medical Imaging, vol. 17, pp. 715-728, 1998.

Copyright 2021 R. H. Taylor

Engineering Research Center for Computer Integrated Surgical Systems and Technology



25

Robust M-Estimator ...

(Following development in Guezic et al., 1998)

Step 3.0: Set $\bar{\mathbf{u}} = \bar{\mathbf{0}}$, $\Delta \bar{\mathbf{t}} = \bar{\mathbf{0}}$

Step 3.1: Compute $e_i = \|\mathbf{V}_i(\bar{\mathbf{p}}_i - \bar{\mathbf{c}}_i + 2\mathbf{P}_i\bar{\mathbf{u}} + \Delta \bar{\mathbf{t}})\|$, $s = \text{median}(\{\dots, e_i, \dots\}) / 0.6745$,

Step 3.2: Solve $\mathbf{C}\bar{\mathbf{x}} = \bar{\mathbf{d}}$, where $\bar{\mathbf{x}}^t = [\bar{\mathbf{u}}^t, \bar{\mathbf{t}}^t]$

$$\mathbf{C} = \sum_i \Psi \left(\frac{e_i}{s} \right) \begin{bmatrix} 2\mathbf{P}_i\mathbf{W}_i\mathbf{P}_i & \mathbf{P}_i\mathbf{W}_i \\ 2\mathbf{P}_i\mathbf{W}_i & \mathbf{W}_i \end{bmatrix} \quad \text{and} \quad \bar{\mathbf{d}} = \sum_i \Psi \left(\frac{e_i}{s} \right) \begin{bmatrix} \mathbf{P}_i\mathbf{W}_i(\bar{\mathbf{c}}_i - \bar{\mathbf{p}}_i) \\ \mathbf{W}_i(\bar{\mathbf{c}}_i - \bar{\mathbf{p}}_i) \end{bmatrix}$$

$$\text{where } \mathbf{W}_i = \mathbf{V}_i^t \mathbf{V}_i = \mathbf{I} - \bar{\mathbf{v}}_i \bar{\mathbf{v}}_i^t \quad \Psi(\mu) = \begin{cases} \mu(1 - \mu^2 / \alpha^2)^2 & \text{if } \|\mu\| \leq \alpha \\ 0 & \text{otherwise} \end{cases}$$

(Note : We use $\alpha=2$)

Step 3.3: Iterate steps 3.1 and 3.2 until a suitable termination condition is reached.

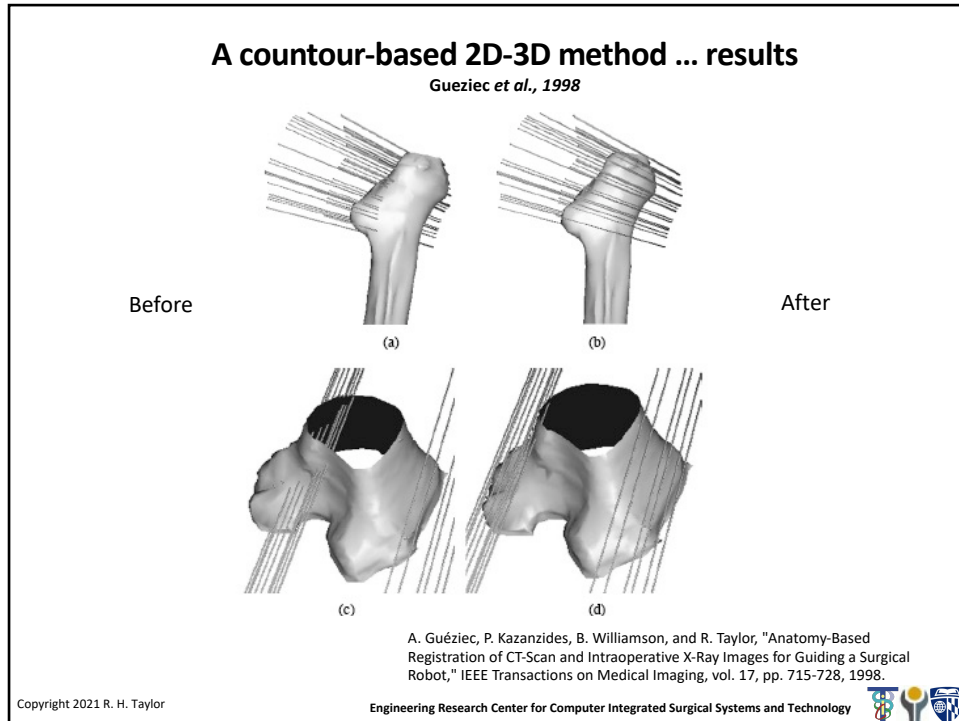
A. Guéziec, P. Kazanzides, B. Williamson, and R. Taylor, "Anatomy-Based Registration of CT-Scan and Intraoperative X-Ray Images for Guiding a Surgical Robot," IEEE Transactions on Medical Imaging, vol. 17, pp. 715-728, 1998.

Copyright 2021 R. H. Taylor

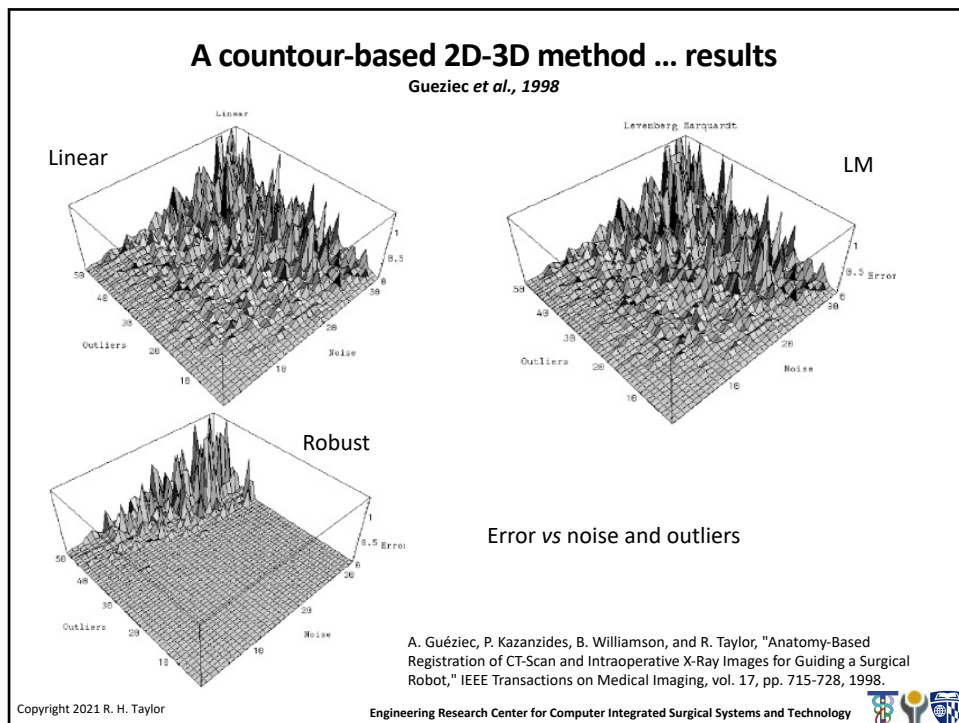
Engineering Research Center for Computer Integrated Surgical Systems and Technology



26



27



28

A contour-based 2D-3D method ... times

Guezic *et al.*, 1998

TABLE I
AVERAGE EXECUTION TIMES IN MS FOR THE THREE
REGISTRATION METHODS APPLIED TO DATA SETS THAT
COMPRISE 100 POINTS (TOP) AND 20 POINTS (BOTTOM)

Number Points/Method	LM	Linear	Robust
100 points (CPU time)	790	690	28
20 points (CPU time)	200	42	9.6

A. Guéziec, P. Kazanzides, B. Williamson, and R. Taylor, "Anatomy-Based Registration of CT-Scan and Intraoperative X-Ray Images for Guiding a Surgical Robot," IEEE Transactions on Medical Imaging, vol. 17, pp. 715-728, 1998.

Copyright 2021 R. H. Taylor

Engineering Research Center for Computer Integrated Surgical Systems and Technology



29

Sample Set Analysis

- **Question:** How good is a particular set of 3D sample points for the purpose of registration to a 3D surface?
- Long line of authors have looked at this question
- Next few slides are based on the work of David Simon, et al (1995)

Copyright 2021 R. H. Taylor

Engineering Research Center for Computer Integrated Surgical Systems and Technology



33

Sample Set Analysis: Distance Estimates

Let

$$F(\mathbf{x}) = 0$$

be the implicit equation of a surface, then one good estimate of the distance of a point \mathbf{x} to the surface is

$$D(\mathbf{x}) = \frac{F(\mathbf{x})}{\|\nabla F(\mathbf{x})\|}$$

Copyright 2021 R. H. Taylor

Engineering Research Center for Computer Integrated Surgical Systems and Technology



34

Sample set analysis: sensitivity

Let \mathbf{x}_s be a point on the surface, and let $T(\bar{\eta})$ represent a small perturbation with parameters $\bar{\eta}$ with respect to the surface of point \mathbf{x}_s :

$$\mathbf{x}'_s = T(\bar{\eta})\mathbf{x}_s$$

Then we define $\mathbf{V}(\mathbf{x}_s)$ to be

$$\mathbf{V}(\mathbf{x}_s) = \frac{\partial D(T(\bar{\eta})\mathbf{x}_s)}{\partial \bar{\eta}} = \begin{bmatrix} \mathbf{n}_s \\ \mathbf{x}_s \times \mathbf{n}_s \end{bmatrix}$$

where \mathbf{n}_s is the unit normal to the surface at \mathbf{x}_s . So,

$$D(T(\bar{\eta})\mathbf{x}_s) \simeq \mathbf{V}^T(\mathbf{x}_s)\bar{\eta}$$

Squaring this gives

$$\begin{aligned} D^2(T(\bar{\eta})\mathbf{x}_s) &\simeq \bar{\eta}^T \mathbf{V}(\mathbf{x}_s) \mathbf{V}^T(\mathbf{x}_s) \bar{\eta} \\ &= \bar{\eta}^T \mathbf{M}(\mathbf{x}_s) \bar{\eta} \end{aligned}$$

Note that \mathbf{M} is 6×6 positive, semi-definite, symmetric matrix.

Copyright 2021 R. H. Taylor

Engineering Research Center for Computer Integrated Surgical Systems and Technology



35

Sample set analysis: sensitivity

For a region \mathcal{R} , define

$$\begin{aligned} E_R(\bar{\eta}) &= \bar{\eta}^T \left[\sum_{\mathbf{x}_s \in \mathcal{R}} \mathbf{M}(\mathbf{x}_s) \right] \bar{\eta} \\ &= \bar{\eta}^T \Psi_{\mathcal{R}} \bar{\eta} \\ &= \bar{\eta}^T \mathbf{Q} \Lambda \mathbf{Q}^T \bar{\eta} \\ &= \sum_{1 \leq i \leq 6} \lambda_i (\bar{\eta}^T \cdot \mathbf{q}_i)^2 \end{aligned}$$

- Note that the eigenvectors \mathbf{q}_i correspond to small differential transformations $\mathbf{T}(\mathbf{q}_i)$, and can sort eigenvalues so that

$$\lambda_1 \geq \lambda_2 \geq \dots \geq \lambda_6$$

- Note that eigenvector \mathbf{q}_1 corresponds to direction of greatest constraint.
- Similarly, can also think of \mathbf{q}_6 as the least constrained direction.

Copyright 2021 R. H. Taylor

hnology 

36

Sample Set Analysis: Goodness Measures


- Magnitude of smallest eigenvalue (Simon)
- (Kim and Khosla)

$$\frac{\sqrt[6]{\lambda_1 \cdot \dots \cdot \lambda_6}}{\lambda_1 + \dots + \lambda_6}$$

- Nahvi

$$\frac{\lambda_6^2}{\lambda_1}$$

Copyright 2021 R. H. Taylor

Engineering Research Center for Computer Integrated Surgical Systems and Technology 

37

Sample Set Selection

- One blind search method (similar to Simon, 1995) is:
 - Randomly select sample points on surface
 - (prune for reachability)
 - evaluate goodness of sample set using some criterion
 - repeat many times and choose the best one found

Copyright 2021 R. H. Taylor

Engineering Research Center for Computer Integrated Surgical Systems and Technology



38

Sample Set Selection

- Refinement of blind search (hill climbing):
 - Randomly select sample points on surface
 - (prune for reachability)
 - evaluate goodness of sample set using some criterion
 - replace a point from sample set with a randomly selected point
 - evaluate goodness
 - if better, keep it
 - else revert to original point and try again
- Variations include simulated annealing, “genetic” algorithms

Copyright 2021 R. H. Taylor

Engineering Research Center for Computer Integrated Surgical Systems and Technology



39

Sample Set Selection: Another Alternative

- Select large number of random points \mathbf{x}_s
- Prune for reachability
- For each point, compute constraint direction $\mathbf{V}_s = \mathbf{V}(\mathbf{x}_s)$. To a first approximation, a measurement at \mathbf{x}_s with accuracy ϵ_s constrains $\bar{\eta}$ by

$$|\mathbf{V}_s \bar{\eta}| \leq \epsilon_s$$

- Now select subset of the \mathbf{x}_s that minimizes, e.g.,

$$\min_{\delta_s} \max \bar{\eta}^T \mathbf{S} \bar{\eta}$$

subject to

$$\begin{aligned} \delta_s &\in \{0, 1\} \\ |\delta_s \mathbf{V}_s \bar{\eta}| &\leq \epsilon_s \\ \sum_s \delta_s &\leq \text{subsetSize} \end{aligned}$$

There are various ways to do this.

Copyright 2021 R. H. Taylor

Engineering Research Center for Computer Integrated Surgical Systems and Technology



40

Sample Set Selection: Another Alternative (con'd)

- One can also minimize other forms, e.g.,

$$\min_s \max_i |\sigma_i \eta_i|$$

subject to similar constraints

- An alternative is to minimize the number of sample points required to ensure that some constraints on $\bar{\eta}$ are guaranteed to be met. E.g.,

$$\min_{\delta_s} \sum \delta_s$$

such that

$$\begin{aligned} \delta_s &\in \{0, 1\} \\ \xi &\leq \xi_{limit} \end{aligned}$$

where

$$\xi = \max_{\bar{\eta}} \bar{\eta}^T \mathbf{S} \bar{\eta}$$

or some other form subject to

$$|\delta_s \mathbf{V}_s \bar{\eta}| \leq \epsilon_s$$

Copyright 2021 R. H. Taylor

Engineering Research Center for Computer Integrated Surgical Systems and Technology



41

Probabilistic Registration

- Registration methods typically use some optimization algorithm to find a “best” transformation between one data set and the other.
- It makes sense to try to find the “most likely” registration transformation.
- ICP minimizes sum-of-squares distances.
- This is equivalent to assuming that point-pair match probabilities are independent and symmetric Gaussian distributions based on distances
- But there are a number of other methods that explicitly consider probabilities ...

Copyright 2021 R. H. Taylor

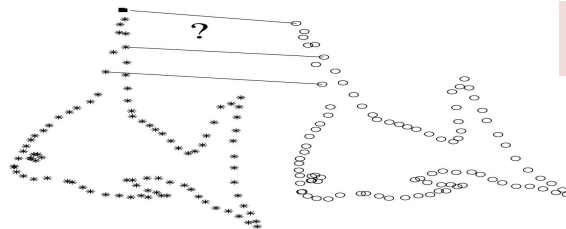
Engineering Research Center for Computer Integrated Surgical Systems and Technology



42

Coherent Point Drift

- A. Myronenko and X. Song, "Point-Set Registration: Coherent Point Drift", *IEEE Trans. on Pattern Analysis and Machine Intelligence*, vol. 32- 12, pp. 2262-2275, 2010.
- Alignment of point clouds
 - Fast method follows “EM” paradigm
 - Tolerates outliers and noise
 - Transformations: Rigid, affine, general deformable



Click here
for [slides](#)

Copyright 2021 R. H. Taylor

Engineering Research Center for Computer Integrated Surgical Systems and Technology

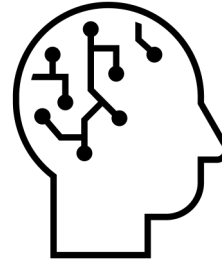


43

Quiz

- The link will be in the chat
- You have 2 minutes

????



Copyright 2021 R. H. Taylor

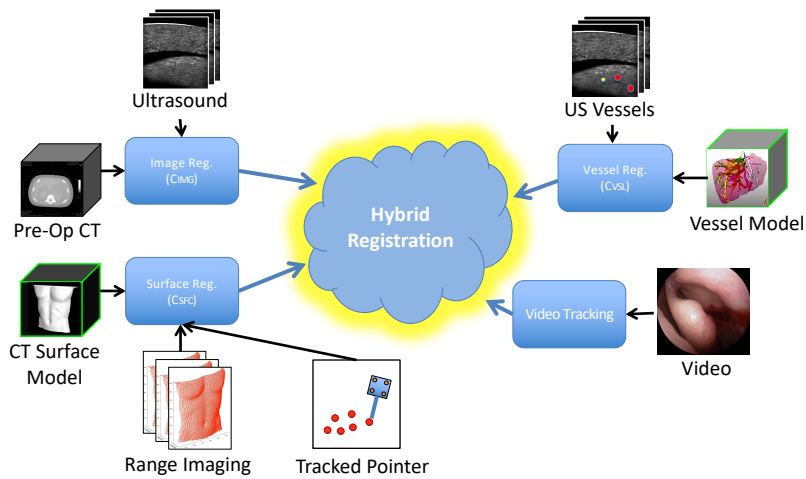
Engineering Research Center for Computer Integrated Surgical Systems and Technology



44

Multi-Modal Feature-Based Registration

Question: How to combine multiple data sources, in order to improve the accuracy and robustness of registration outcomes?

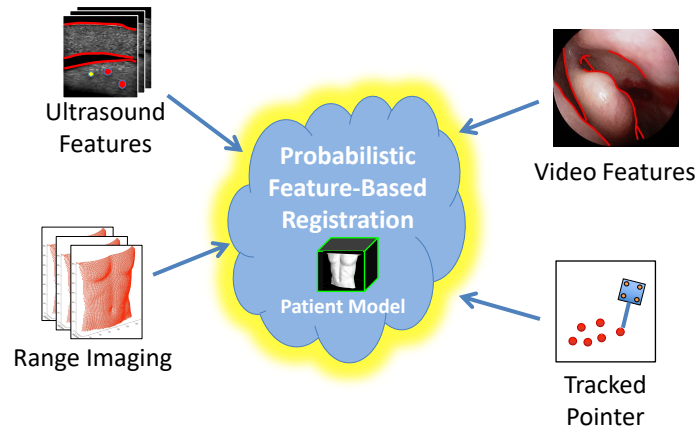


Billings S, Kapoor A, Keil M, Wood BJ, Boctor E (2011) A Hybrid Surface/Image-Based Approach to Facilitate Ultrasound/CT Registration. In: *SPIE, Medical Imaging 2011: Ultrasonic Imaging, Tomography, and Therapy*

47

Multi-Modal Feature-Based Registration

Question: How to combine multiple data sources, in order to improve the accuracy and robustness of registration outcomes?



Copyright 2021 R. H. Taylor

Credit: Seth Billings Engineering Research Center for Computer Integrated Surgical Systems and Technology



48

Iterative Closest Point (ICP) Revisited

- Widely popular and useful method for point cloud to surface registration introduced by Besl & McKay in 1992
- Many variants proposed since its inception affecting all aspects of the algorithm (robustness, matching criteria, match alignment, etc.)

➤ Matching Phase:

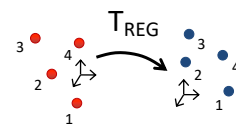
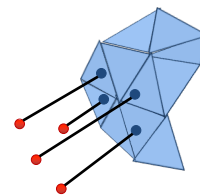
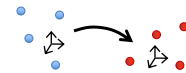
for each point in the source shape, find the closest point on the target shape

$$\mathbf{y}_i = C_{CP}(T(\mathbf{x}_i), \Psi) = \operatorname{argmin}_{\mathbf{y} \in \Psi} \|\mathbf{y} - T(\mathbf{x}_i)\|_2$$

➤ Registration Phase:

compute transformation to minimize sum of square distances between matches

$$T = \operatorname{argmin}_T \sum_{i=1}^n \|\mathbf{y}_i - T(\mathbf{x}_i)\|_2^2$$



S. Billings and R. H. Taylor, "Iterative Most Likely Oriented Point Registration", in *Medical Image Computing and Computer-Assisted Interventions (MICCAI)*, Boston, October, 2014.

Copyright 2021 R. H. Taylor

Credit: Seth Billings Engineering Research Center for Computer Integrated Surgical Systems and Technology



49

Most-Likely Point Paradigm Illustrated with ICP

- 1. Probability Model:** isotropic Gaussian

$$f_{\text{match}}(\mathbf{x} | \mathbf{y}, \sigma^2) = \frac{1}{(2\pi\sigma^2)^{3/2}} \cdot e^{-\frac{1}{2\sigma^2} \|\mathbf{y} - \mathbf{x}\|^2}$$

- 2. Match Phase:**

$$\begin{aligned} \mathbf{y}_i &= \operatorname{argmax}_{\mathbf{y}_i \in \mathcal{Y}} f_{\text{match}}(\mathbf{T}(\mathbf{x}_i) | \mathbf{y}_i, \sigma^2) \\ &= \operatorname{argmax}_{\mathbf{y}_i \in \mathcal{Y}} \frac{1}{(2\pi\sigma^2)^{3/2}} \cdot e^{-\frac{1}{2\sigma^2} \|\mathbf{y}_i - \mathbf{T}(\mathbf{x}_i)\|^2} \\ &\rightarrow \operatorname{argmin}_{\mathbf{y}_i \in \mathcal{Y}} \|\mathbf{y}_i - \mathbf{T}(\mathbf{x}_i)\| \end{aligned}$$

- 3. Registration Phase:**

$$\begin{aligned} \mathbf{T} &= \operatorname{argmax}_{\mathbf{T}} \prod_i^n f_{\text{match}}(\mathbf{T}(\mathbf{x}_i) | \mathbf{y}_i, \sigma^2) \\ &= \operatorname{argmax}_{\mathbf{T}} \prod_i^n \frac{1}{(2\pi\sigma^2)^{3/2}} \cdot e^{-\frac{1}{2\sigma^2} \|\mathbf{y}_i - \mathbf{T}(\mathbf{x}_i)\|^2} \\ &\rightarrow \operatorname{argmax}_{\mathbf{T}} \left[-n \log \left((2\pi\sigma^2)^{3/2} \right) - \frac{1}{2\sigma^2} \sum_i^n \|\mathbf{y}_i - \mathbf{T}(\mathbf{x}_i)\|^2 \right] \\ &\rightarrow \operatorname{argmin}_{\mathbf{T}} \sum_i^n \|\mathbf{y}_i - \mathbf{T}(\mathbf{x}_i)\|^2 \end{aligned}$$

Copyright 2021 R. H. Taylor

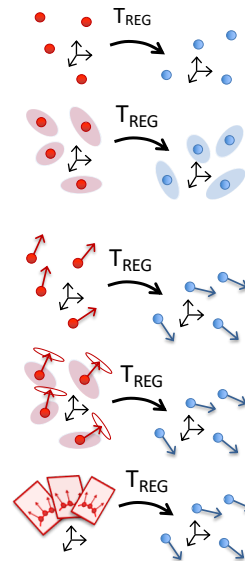
Credit: Seth Billing Engineering Research Center for Computer Integrated Surgical Systems and Technology



50

Outline of Registration Algorithms

- ICP - Iterative Closest Point
 - isotropic position data
- **IMLP - Iterative Most Likely Point**
 - anisotropic position data
 - robust to outliers
- IMLOP - Iterative Most Likely Oriented Point
 - isotropic position & orientation data
- G-IMLOP - Generalized IMLOP
 - anisotropic position & orientation data
- P-IMLOP - Projected IMLOP
 - anisotropic position & projected orientation data



Copyright 2021 R. H. Taylor

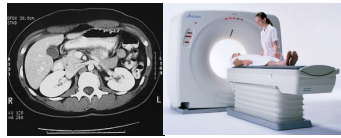
Credit: Seth Billing Engineering Research Center for Computer Integrated Surgical Systems and Technology



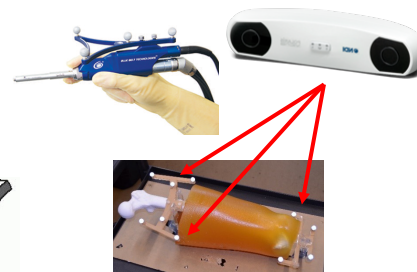
52

Sources of Anisotropic Uncertainty

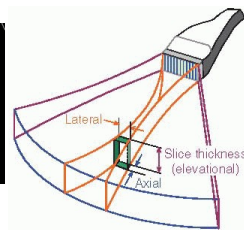
Tomographic Imaging



Stereo Vision



Ultrasound



Figures: http://www.ndt-intel.com/wp-content/uploads/2013/09/4col_polarisvcr3.png; The Essential Physics of Medical Imaging, 2nd Ed.; https://www.infotech.edu.au/wp-content/uploads/2013/01/L_A_B_Look-At-Baby-3D-Ultrasound-Tests-Ultrasound-Technicians-hw-300x225.jpg; http://001.lalimg.com/photo/v0/105832128/CT_Scan_equipment.jpg

Copyright 2021 R. H. Taylor

Credit: Seth Billing Engineering Research Center for Computer Integrated Surgical Systems and Technology



53

Prior Work: Anisotropic Registration

- Generalized Total Least Squares ICP (GTLS-ICP)
 - Estépar RSJ, Brun A, Westin C-F (2004) Robust generalized total least squares iterative closest point registration. In: *MICCAI 2004*
 - Registration Phase
 - **anisotropic** noise model
 - ad-hoc implementation **less accurate / efficient**; can be **unstable**
 - Match Phase
 - **isotropic** (i.e. closest-point matching)
- Generalized ICP (G-ICP)
 - Registration Phase
 - **anisotropic** noise model **limited** to model locally-linear surface regions surrounding each feature point of a point cloud shape
 - uses off-the-shelf conjugate gradient solver
 - Match Phase
 - **isotropic** (i.e. closest-point matching)

Segal A, Haehnel D, Thrun S (2009) Generalized-ICP. In: *Robotics: Science and Systems V*

Copyright 2021 R. H. Taylor

Credit: Seth Billing Engineering Research Center for Computer Integrated Surgical Systems and Technology



54

Prior Work: Anisotropic Registration

- Anisotropic ICP (A-ICP)

Maier-Hein L, Franz AM, Dos Santos TR, Schmidt M, Fangerau M, et al. (2012) Convergent iterative closest-point algorithm to accommodate anisotropic and inhomogeneous localization error. *IEEE Trans Pattern Anal Mach Intell* 34: 1520–1532.

- Registration Phase

- anisotropic noise model
- ad-hoc implementation **does not fully account** for noise in both shapes (i.e., lacks ability to reorient the data-shape covariances during optimization)

- Match Phase

- anisotropic noise model with **non-optimal matching** (finds minimal Mahalanobis distance match rather than most-likely match)
- **inefficient** implementation; also **cannot guarantee** that the “best” match is found

- **Initializes registration by ICP** (due to inefficient match phase)

Copyright 2021 R. H. Taylor

Credit: Seth Billings

Engineering Research Center for Computer Integrated Surgical Systems and Technology



55

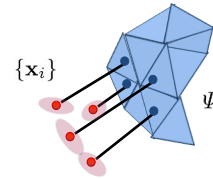
Iterative Most Likely Point (IMLP)

Probability Model: anisotropic Gaussian

$$f_{\text{match}}(\mathbf{x} | \mathbf{y}, \Sigma_{\mathbf{x}}, \Sigma_{\mathbf{y}}) = \frac{1}{(2\pi)^{3/2} |\Sigma_{\mathbf{x}} + \Sigma_{\mathbf{y}}|^{1/2}} \cdot e^{-\frac{1}{2}(\mathbf{y} - \mathbf{x})^T (\Sigma_{\mathbf{x}} + \Sigma_{\mathbf{y}})^{-1} (\mathbf{y} - \mathbf{x})}$$

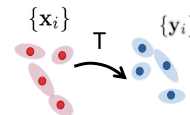
Match Phase:

$$[\mathbf{y}_i, \Sigma_{\mathbf{y}_i}] = \underset{[\mathbf{y}_i, \Sigma_{\mathbf{y}_i}] \in \Psi}{\operatorname{argmin}} \left[\log(|\mathbf{R}\Sigma_{\mathbf{x}_i}\mathbf{R}^T + \Sigma_{\mathbf{y}_i}|) + (\mathbf{y}_i - \mathbf{T}(\mathbf{x}_i))^T (\mathbf{R}\Sigma_{\mathbf{x}_i}\mathbf{R}^T + \Sigma_{\mathbf{y}_i})^{-1} (\mathbf{y}_i - \mathbf{T}(\mathbf{x}_i)) \right]$$



Registration Phase:

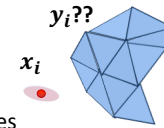
$$\mathbf{T} = \underset{\mathbf{T}=[\mathbf{R}, \mathbf{t}]}{\operatorname{argmin}} \sum_i^n (\mathbf{y}_i - \mathbf{T}(\mathbf{x}_i))^T (\mathbf{R}\Sigma_{\mathbf{x}_i}\mathbf{R}^T + \Sigma_{\mathbf{y}_i})^{-1} (\mathbf{y}_i - \mathbf{T}(\mathbf{x}_i))$$



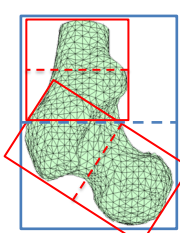
Billings SD, Bocker EM, Taylor RH (2015) Iterative Most-Likely Point Registration (IMLP): A Robust Algorithm for Computing Optimal Shape Alignment. *PLoS One* 10: e0117688

56

IMLP: Match Phase



- Due to anisotropic distance metric, standard KD-tree search techniques do not apply.
- **Approach:** PD-tree search with modified node test



PD Tree Constructed by Datum Positions

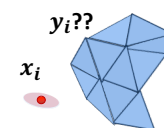
Constructing the PD tree:

1. Add all datums to a root node
2. Compute covariance of datum positions within the node
3. Create minimally-sized bounding box aligned to the covariance eigenvectors
4. Partition node along the direction of greatest extent
5. Form left and right child nodes from the datums in each partition
6. Repeat from Step 2 for left and right child nodes until # datums in node < threshold or node size < threshold

Copyright 2021 R. H. Taylor Credit: Seth BillingEngineering Research Center for Computer Integrated Surgical Systems and Technology

57

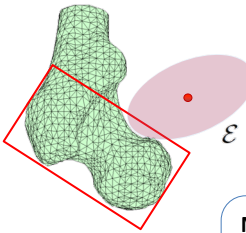
IMLP: Match Phase



Searching the PD tree:

Assume the **current match candidate** has a match error equal to E_{best}

Question: can any feature in this node possibly provide a match error less than E_{best} ?



Node of the PD Tree

$$[y_i, \Sigma_{y_i}] = \operatorname{argmin}_{[y_i, \Sigma_{y_i}] \in \Psi} \left[\log(\mathbf{R}\Sigma_{x_i}\mathbf{R}^T + \Sigma_{y_i}) + (y_i - T(x_i))^T (\mathbf{R}\Sigma_{x_i}\mathbf{R}^T + \Sigma_{y_i})^{-1} (y_i - T(x_i)) \right]$$

True if: $(y_i - T(x_i))^T (\mathbf{R}\Sigma_{x_i}\mathbf{R}^T + \Sigma_{node})^{-1} (y_i - T(x_i)) < E_{best} - \log_{min}$

Node Test: if the **ellipsoid**

$$\mathcal{E} = \{y \mid (y - T(x_i))^T (\mathbf{R}\Sigma_{x_i}\mathbf{R}^T + \Sigma_{node})^{-1} (y - T(x_i)) \leq E_{best} - \log_{min}\}$$

intersects the bounding box of the node, then search the node

Copyright 2021 R. H. Taylor Credit: Seth BillingEngineering Research Center for Computer Integrated Surgical Systems and Technology

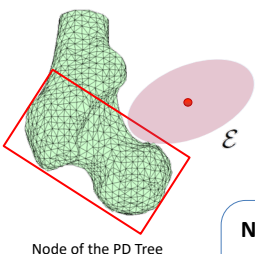
58

IMLP: Match Phase

Searching the PD tree:

Assume the **current match candidate** has a match error equal to E_{best}

Question: can any feature in this node possibly provide a match error less than E_{best} ?



$$[y_i, \Sigma_{y_i}] = \underset{[y_i, \Sigma_{y_i}] \in \Psi}{\operatorname{argmin}} \left[\log(\mathbf{R}\Sigma_{x_i}\mathbf{R}^T + \Sigma_{y_i}) + (y_i - \mathbf{T}(x_i))^T (\mathbf{R}\Sigma_{x_i}\mathbf{R}^T + \Sigma_{y_i})^{-1} (y_i - \mathbf{T}(x_i)) \right]$$

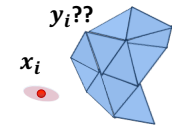
True if: $(y_i - \mathbf{T}(x_i))^T (\mathbf{R}\Sigma_{x_i}\mathbf{R}^T + \Sigma_{node})^{-1} (y_i - \mathbf{T}(x_i)) < E_{best} - \log_{min}$

Details in Billings' Thesis

Node Test: if the **ellipsoid**

$$\mathcal{E} = \{y \mid (y - \mathbf{T}(x_i))^T (\mathbf{R}\Sigma_{x_i}\mathbf{R}^T + \Sigma_{node})^{-1} (y - \mathbf{T}(x_i)) \leq E_{best} - \log_{min}\}$$

intersects the bounding box of the node, then search the node



Copyright 2021 R. H. Taylor Credit: Seth Billings Engineering Research Center for Computer Integrated Surgical Systems and Technology

59

IMLP: Registration Phase

1. Re-formulate the cost function from an unconstrained optimization

$$\mathbf{T} = \underset{[\mathbf{R}, \mathbf{t}]}{\operatorname{argmin}} \sum_{i=1}^n (y_i - \mathbf{R}x_i - \mathbf{t})^T (\mathbf{R}\Sigma_{x_i}\mathbf{R}^T + \Sigma_{y_i})^{-1} (y_i - \mathbf{R}x_i - \mathbf{t})$$

to a constrained optimization

$$\mathbf{T} = \underset{[\mathbf{R}, \mathbf{t}]}{\operatorname{argmin}} \sum_{i=1}^n (x_i - x_i^*)^T \Sigma_{x_i}^{-1} (x_i - x_i^*) + \sum_{i=1}^n (y_i - y_i^*)^T \Sigma_{y_i}^{-1} (y_i - y_i^*)$$

subject to: $F_i(x_i^*, y_i^*, \mathbf{R}, \mathbf{t}) = y_i^* - \mathbf{R}x_i^* - \mathbf{t} = 0$

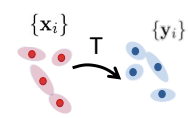
x_i^* - true (unknown) data-point position
 y_i^* - true (unknown) model-point position

2. **Linearize** the constraints with a **Taylor series** centered at the measured (known) data

$$F_i(x_i^*, y_i^*, \mathbf{R}, \mathbf{t}) \approx F_{L_i}^k(x_i, y_i, \mathbf{d}\alpha, \mathbf{d}\mathbf{t})$$

$$= F_i^0(x_i, y_i, \mathbf{R}_k, \mathbf{t}_k) - \mathbf{r}_{y_i} + \mathbf{R}_k \mathbf{r}_{x_i} + \operatorname{skew}(\mathbf{R}_k x_i) \mathbf{d}\alpha - \mathbf{d}\mathbf{t} = 0$$

Note using: $\Delta \mathbf{R} \approx \mathbf{I} + \operatorname{skew}(\mathbf{d}\alpha) \quad \mathbf{r}_{x_i} = x_i - x_i^* \quad \mathbf{r}_{y_i} = y_i - y_i^*$



Copyright 2021 R. H. Taylor Credit: Seth Billings Engineering Research Center for Computer Integrated Surgical Systems and Technology

60

IMLP: Registration Phase

3. Apply the method of **Lagrange multipliers** to solve constrained optimization.

3a. Form the **Lagrange function** using the linearized constraints

$$\mathcal{L}(d\alpha, dt, \lambda) = \sum_{i=1}^n \mathbf{r}_{xi}^T \Sigma_{xi}^{-1} \mathbf{r}_{xi} + \sum_{i=1}^n \mathbf{r}_{yi}^T \Sigma_{yi}^{-1} \mathbf{r}_{yi} + \sum_{i=1}^n \lambda_i^T F_{Li}^k(\mathbf{x}_i, \mathbf{y}_i, d\alpha, dt)$$

3b. Solve zero gradient w.r.t. the optimization parameters and the Lagrange multipliers

$$\mathbf{J}^T \Sigma^{-1} \mathbf{J} d\mathbf{p} = -\mathbf{J}^T \Sigma^{-1} \mathbf{f}^0 \quad \text{modified Gauss-Newton}$$

$$d\mathbf{p} = \begin{bmatrix} d\alpha \\ dt \end{bmatrix} \quad \mathbf{f}^0 = \begin{bmatrix} \mathbf{f}_1^0 \\ \vdots \\ \mathbf{f}_n^0 \end{bmatrix} \quad \mathbf{J} = \begin{bmatrix} \text{skew}(\mathbf{R}_k \mathbf{x}_1) & -\mathbf{I} \\ \vdots & \vdots \\ \text{skew}(\mathbf{R}_k \mathbf{x}_n) & -\mathbf{I} \end{bmatrix} \quad \Sigma = \begin{bmatrix} \mathbf{F}_x^0 \Sigma_x \mathbf{F}_x^{0T} + \Sigma_y \end{bmatrix}$$

$$\mathbf{F}_x^0 = \begin{bmatrix} -\mathbf{R}_k & & \\ & \ddots & \\ & & -\mathbf{R}_k \end{bmatrix} \quad \Sigma_x = \begin{bmatrix} \Sigma_{x1} & & \\ & \ddots & \\ & & \Sigma_{xn} \end{bmatrix} \quad \Sigma_y = \begin{bmatrix} \Sigma_{y1} & & \\ & \ddots & \\ & & \Sigma_{yn} \end{bmatrix}$$

4. Iteratively solve 3b by linear least squares until convergence.

$$\mathbf{R}_{k+1} = \mathbf{R}(d\alpha) \mathbf{R}_k, \quad \mathbf{t}_{k+1} = \mathbf{t}_k + dt$$

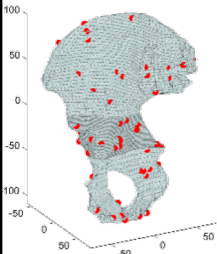
Copyright 2021 R. H. Taylor Credit: Seth Billing Engineering Research Center for Computer Integrated Surgical Systems and Technology

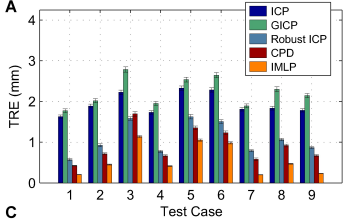
61

IMLP: Experiments

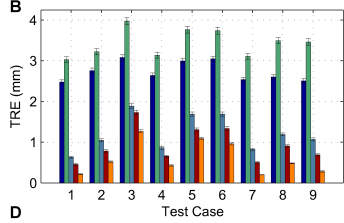
Credit: Seth Billings

- Data Shape:** 100 noisy points + **outliers** simulated from a mesh model of a human hip
- Model Shape:** point-cloud formed from the center points of the mesh triangles
- Random **initial misalignments** [30,60] mm and [30,60] degrees
- Target registration error (TRE) averaged over 300 **randomized trials** for each test case







A



B



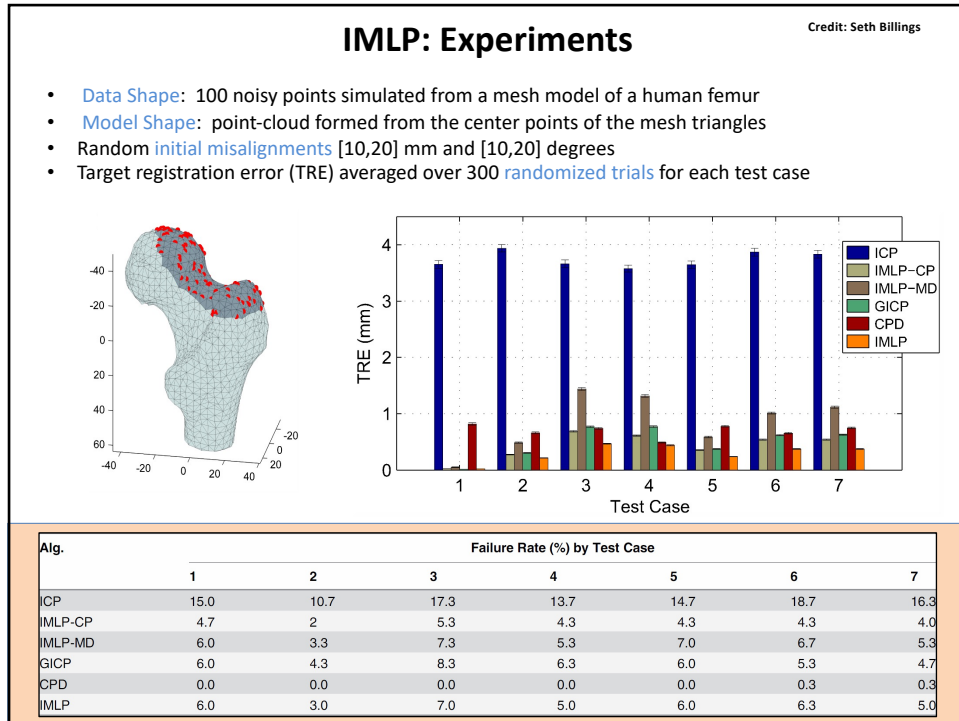
C



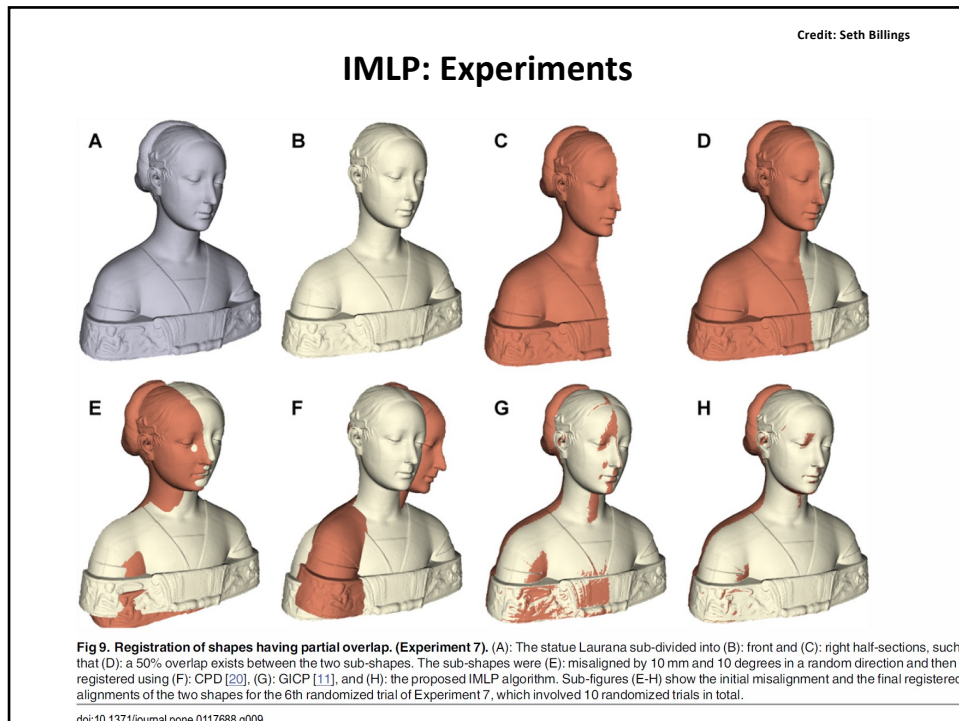
D

Average Runtime (sec.) by Test Case									
Alg	1	2	3	4	5	6	7	8	9
ICP	0.009	0.009	0.010	0.009	0.010	0.009	0.009	0.009	0.009
IMLP-CP	0.015	0.016	0.019	0.016	0.020	0.019	0.015	0.017	0.015
IMLP-MD	0.068	0.078	0.093	0.079	0.097	0.093	0.067	0.079	0.069
GICP	-	-	-	-	-	-	-	-	-
CPD (2 cores)	3.465	4.346	4.336	3.864	4.340	4.374	4.238	4.650	4.484
IMLP	0.068	0.082	0.102	0.078	0.103	0.099	0.067	0.084	0.073

63



64

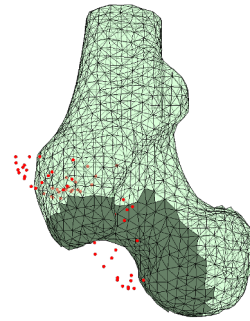


65

Experiments

Performance comparison of IMLOP vs. ICP was made through a simulation study using a human femur surface mesh segmented from CT imaging.

- source shape created by randomly sampling points from the mesh surface (10, 20, 35, 50, 75, and 100 points tested)
- Gaussian [wrapped Gaussian] noise added to the source points (0, 0.5, 1.0, and 2.0 mm [degrees] tested)
- Applied random misalignment of [10,20] mm / degrees
- 300 trials performed for each sample size / noise level
- Registration accuracy (TRE) evaluated using 100 validation points randomly sampled from the mesh
- Registration failures automatically detected using threshold on final residual match errors



Example source point cloud sampled from dark region of target mesh.

ICP: threshold on position residuals only

IMLOP: threshold on position & orientation residuals

S. Billings and R. H. Taylor, "Iterative Most Likely Oriented Point Registration", in *Medical Image Computing and Computer-Assisted Interventions (MICCAI)*, Boston, October, 2014.

Copyright 2021 R. H. Taylor

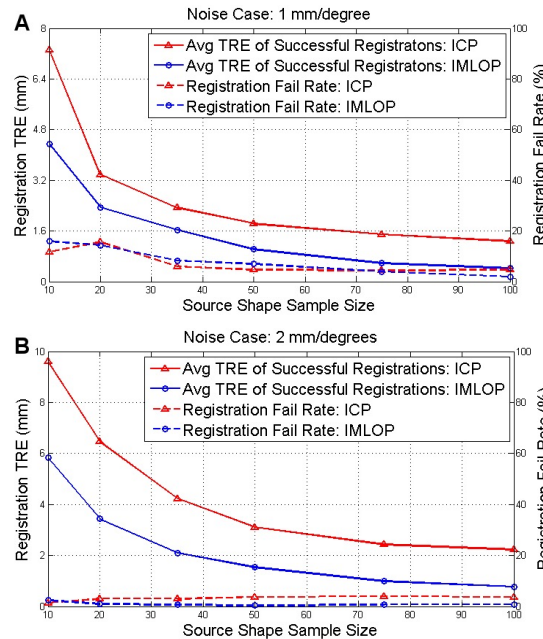
Engineering Research Center for Computer Integrated Surgical Systems and Technology



70

Average TRE of successful registrations and registration failure rates across all sample sizes for noise levels of 1 (A) and 2 (B) mm [degrees].

Registration failure threshold set to twice the noise level for both position and orientation.



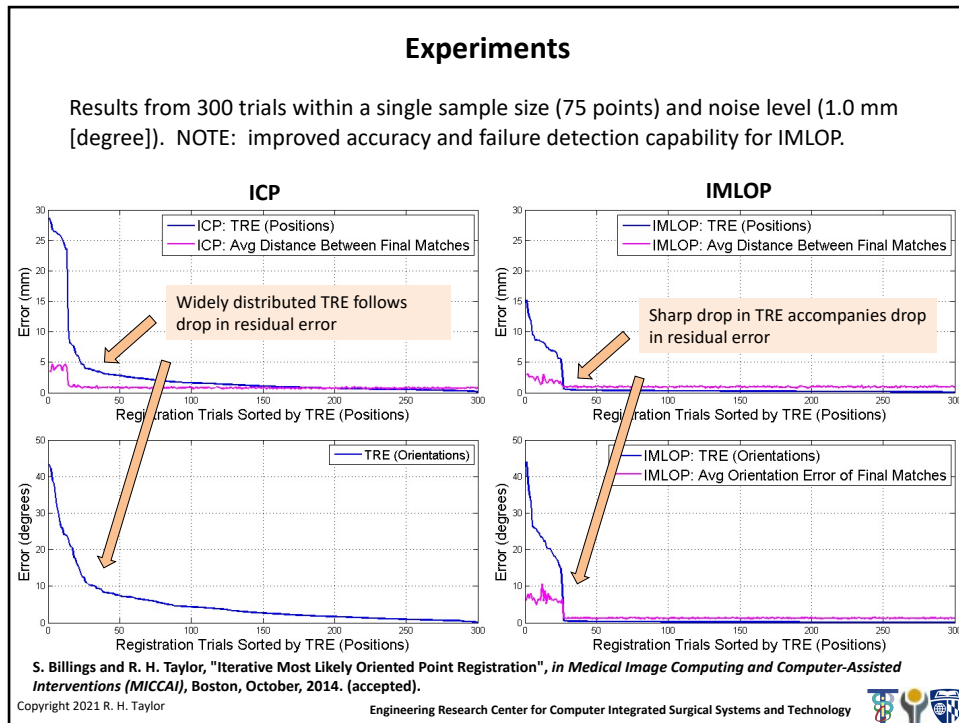
S. Billings and R. H. Taylor, "Iterative Most Likely Oriented Point Registration", in *Medical Image Computing and Computer-Assisted Interventions (MICCAI)*, Boston, October, 2014. (accepted).

Copyright 2021 R. H. Taylor

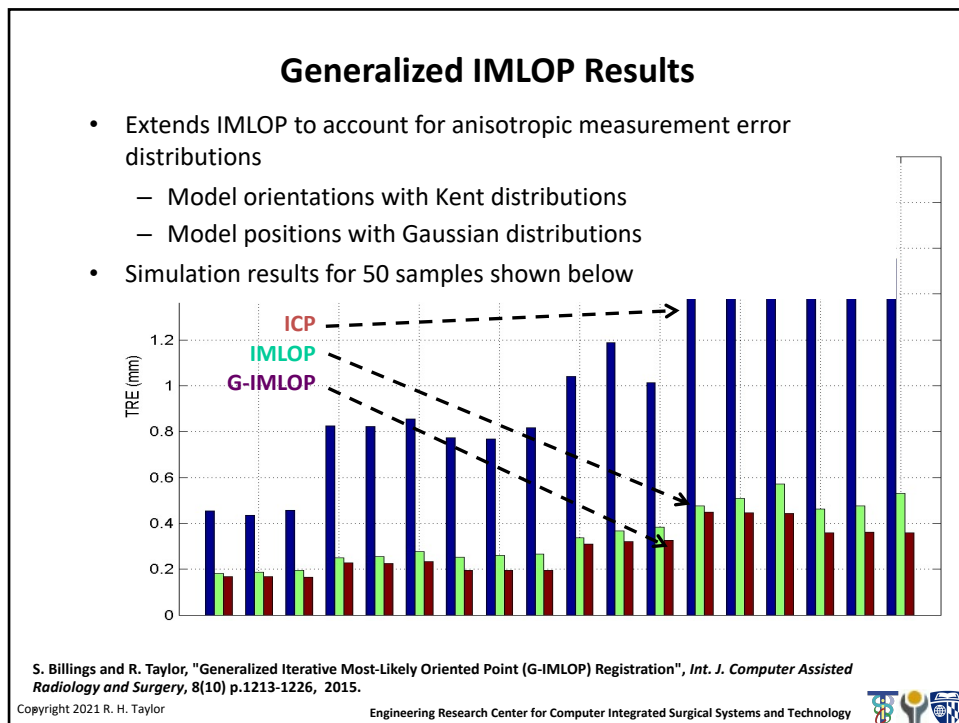
Engineering Research Center for Computer Integrated Surgical Systems and Technology



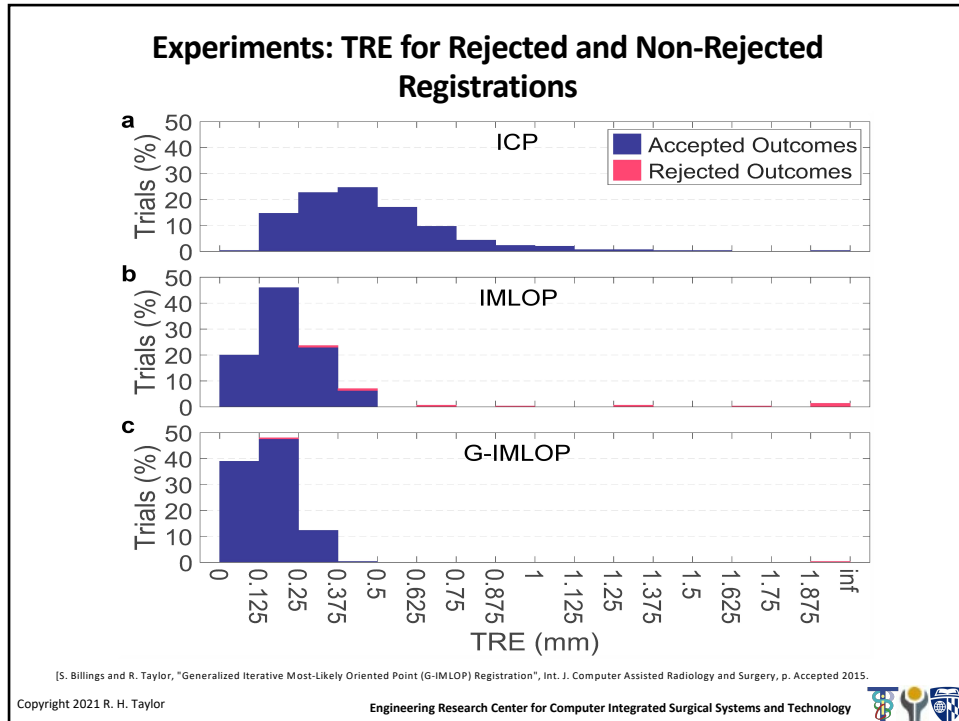
71



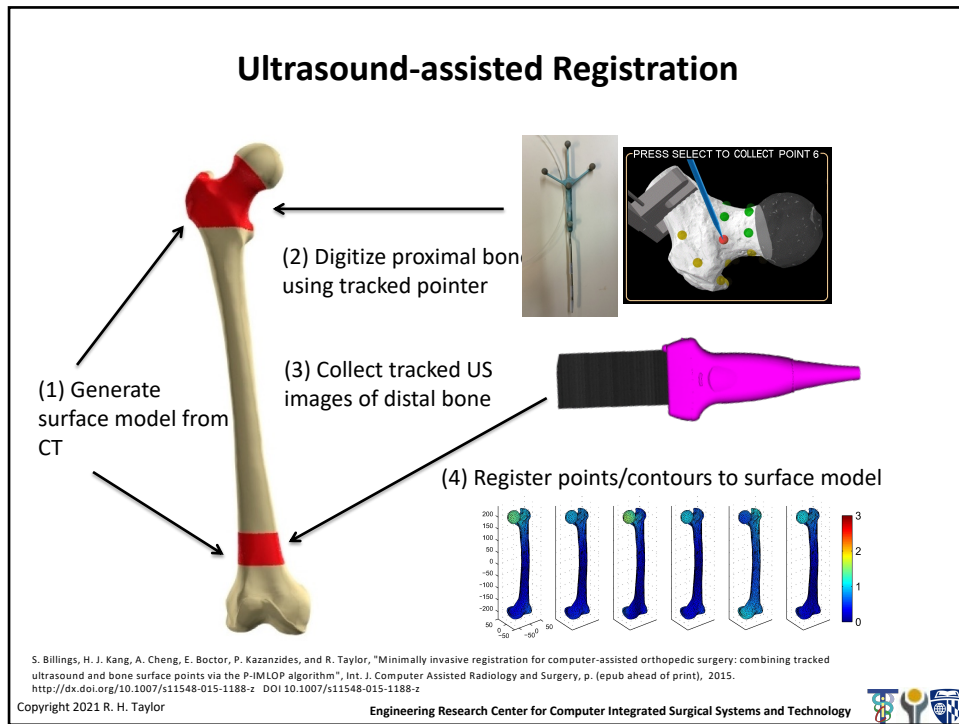
72



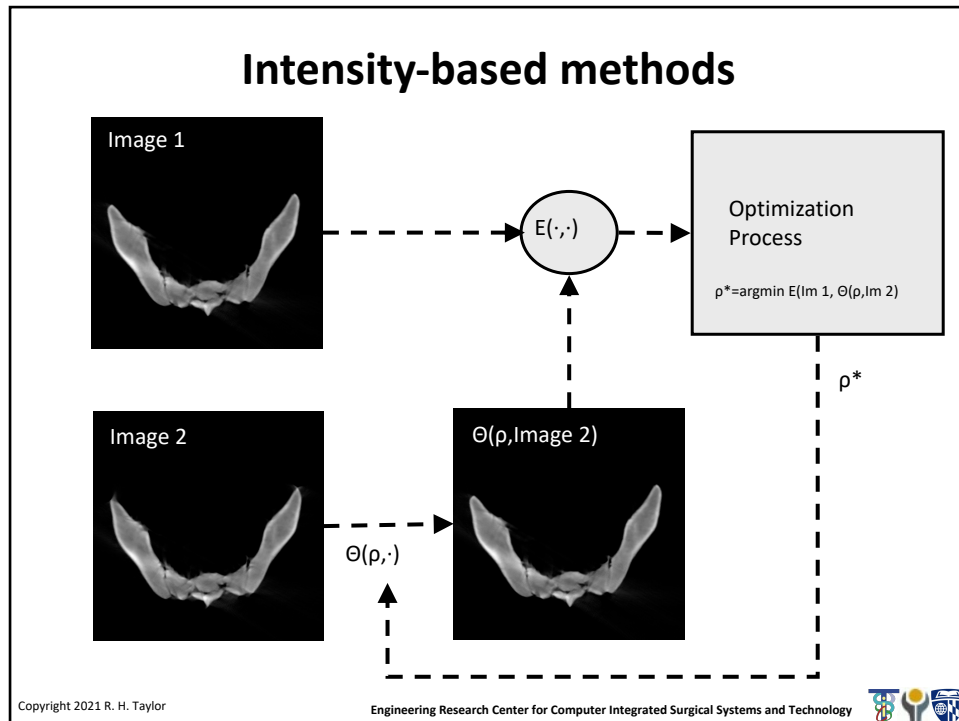
73



74



75



76

Intensity-based methods

- Typically performed between images
- The “features” in this case are the intensities associated with pixels (2D) or voxels (3D) in the images.
- General framework:

$$\vec{\rho}^* = \min_{\vec{\rho}} E\left(\text{Image}_1, \Theta\left(\vec{\rho}, \text{Image}_2\right)\right)$$

- Methods differ mostly in choice of transformation function $\Theta(\cdot)$ and Energy function $E(\cdot, \cdot)$,

Copyright 2021 R. H. Taylor
 Engineering Research Center for Computer Integrated Surgical Systems and Technology

77

Typical energy functions (not an exhaustive list)

Normalized image subtraction

$$E(I_{m_1}, I_{m_2}) = \sum_{\bar{k}} \frac{|I_{m_1}[\bar{k}] - I_{m_2}[\bar{k}]|}{\max_j (|I_{m_1}[\bar{j}] - I_{m_2}[\bar{j}]|)}$$

Normalized cross correlation (NCC)

$$E(I_{m_1}, I_{m_2}) = \frac{\sum_{\bar{k}} (I_{m_1}[\bar{k}] - \text{avg}(I_{m_1})) (I_{m_2}[\bar{k}] - \text{avg}(I_{m_2}))}{\sqrt{\sum_{\bar{k}} (I_{m_1}[\bar{k}] - \text{avg}(I_{m_1}))^2} \sqrt{\sum_{\bar{k}} (I_{m_2}[\bar{k}] - \text{avg}(I_{m_2}))^2}}$$

Mutual information

$$\rightarrow E(I_{m_1}, I_{m_2}) = \sum_{p \in I_{m_1}, q \in I_{m_2}} \Pr(p, q) \log \Pr(p, q) - \Pr_{I_{m_1}}(p) \log \Pr_{I_{m_1}}(p) - \Pr_{I_{m_2}}(q) \log \Pr_{I_{m_2}}(q)$$

Copyright 2021 R. H. Taylor

Engineering Research Center for Computer Integrated Surgical Systems and Technology



78

Mutual Information

- First proposed independently in 1995 by Collignon and Viola & Wells.
- Very widely practiced
- Is able to co-register images with very different sensor modalities so long as there is a stable relationship between intensities in one modality with those in another
- Many “flavors” and variations

Copyright 2021 R. H. Taylor

Engineering Research Center for Computer Integrated Surgical Systems and Technology



79

Mutual Information

Entropy

$$H(a) = \Pr(a) \log \Pr(a)$$

$$H(a,b) = \Pr(a,b) \log \Pr(a,b)$$

Mutual Information (Viola & Wells '95, Colligen '95)

$$\text{Similarity}(A,B) = H(A) + H(B) - H(A,B)$$

Normalized mutual information (Maes *et al.* '97)

$$\text{Similarity}(A,B) = \frac{H(A) + H(B)}{H(A,B)}$$

Objective function

$$E(\text{Im}_1, \text{Im}_2) = -\text{Similarity}(\text{Im}_1, \text{Im}_2)$$

Copyright 2021 R. H. Taylor

Engineering Research Center for Computer Integrated Surgical Systems and Technology

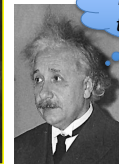
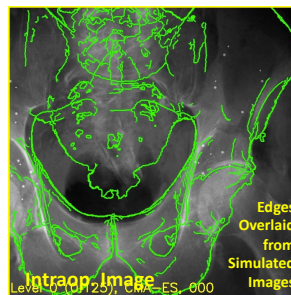
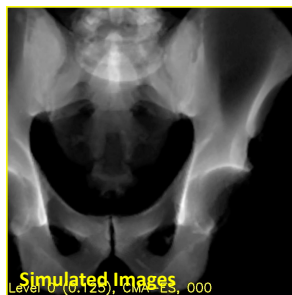


80

Basic Idea of Intensity-Based 2D/3D Registration

- Assumes a pre-op CT is available
- Simulate many C-Arm images and choose the most similar to the intraoperative image
- Solves the following optimization problem:

$$\underset{\theta \in SE(3)}{\text{argmin}} \mathcal{S}(I_{\text{Intra-Op}}, \mathcal{P}(\theta, I_{\text{CT}}))$$



Do these look the same yet?

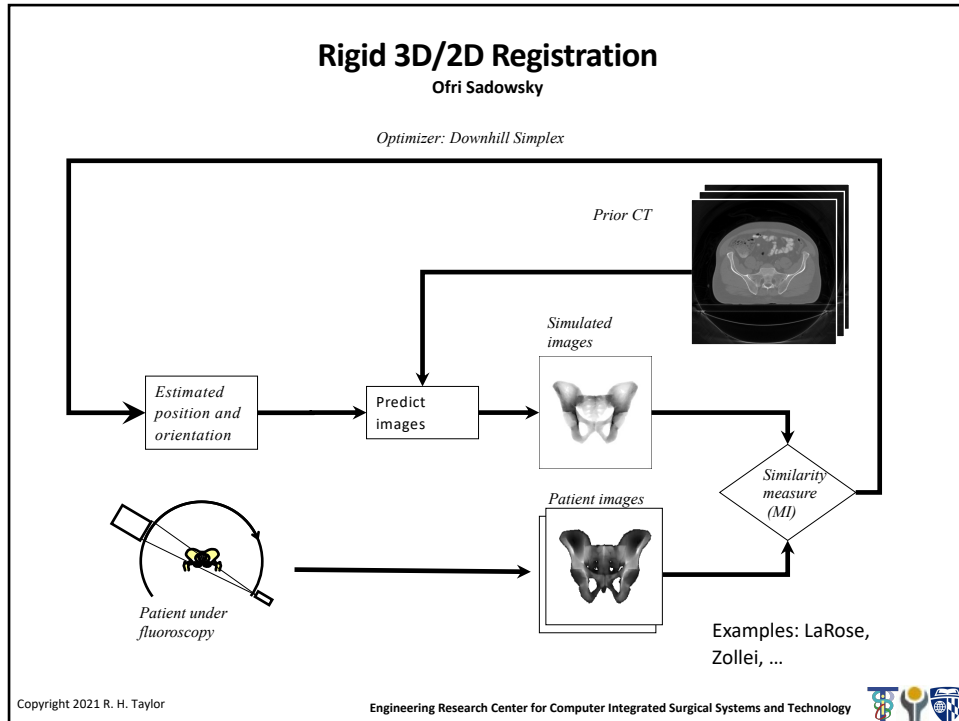
Slide credit: Robert Grupp

Copyright 2021 R. H. Taylor

Engineering Research Center for Computer Integrated Surgical Systems and Technology



81



82

ciis
BACS
Biomechanical and Computer Integrated Surgical Systems Laboratory

A clinical example (periacetabular osteotomy)

Problem: Acetabular Dysplasia

Normal hip bones Hip dysplasia

Image Source: ouh.nhs.uk

Dislocation Caused by Dysplasia

Image Source: James Heilman, MD

Slide credit: Robert Grupp

Engineering Research Center for Computer Integrated Surgical Systems and Technology

84

ciis **BACS**
Biomechanical and Integrated Surgical Systems Laboratory

A clinical example (periacetabular osteotomy)

One Solution: Periacetabular Osteotomy (PAO)

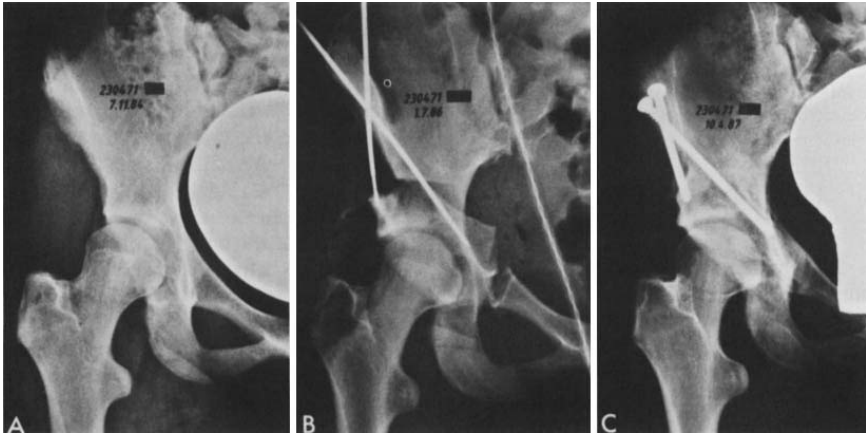


Image Source: Ganz 1988

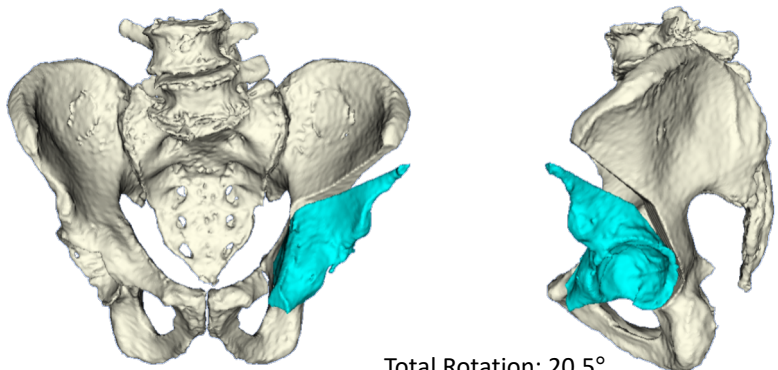
Copyright 2021 R. H. Taylor Slide credit: Robert Grupp Engineering Research Center for Computer Integrated Surgical Systems and Technology

85

ciis **BACS**
Biomechanical and Integrated Surgical Systems Laboratory

A clinical example (periacetabular osteotomy)

Goal: Automatic visualization and guidance



Total Rotation: 20.5°
Anterior/Posterior Rotation: 3.7°
Left/Right Rotation: 16.3°
Inferior/Superior Rotation: 12.5°

Copyright 2021 R. H. Taylor Slide credit: Robert Grupp Engineering Research Center for Computer Integrated Surgical Systems and Technology

86

Movement of the Osteotomy Fragment is Challenging



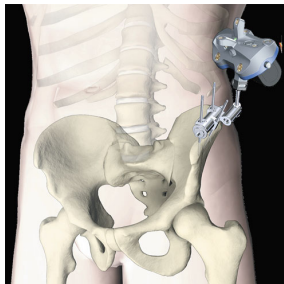
Copyright 2021 R. H. Taylor

Slide credit: Robert Grupp
Engineering Research Center for Computer Integrated Surgical Systems and Technology

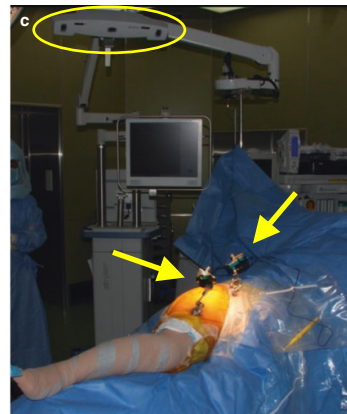


87

One Approach for Computer-Assistance: Optical Tracking Devices



Source: Stiehl and Thornberry, 2016



Source: Sugano, CAOS for Hip and Knee, 2018

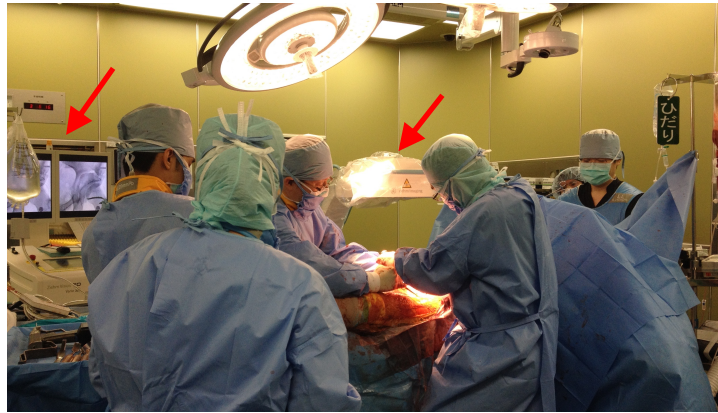
Copyright 2021 R. H. Taylor

Slide credit: Robert Grupp
Engineering Research Center for Computer Integrated Surgical Systems and Technology



88

Intraoperative Fluoroscopy is Available



Chapter 4: Pose Estimation Using Fluoroscopy

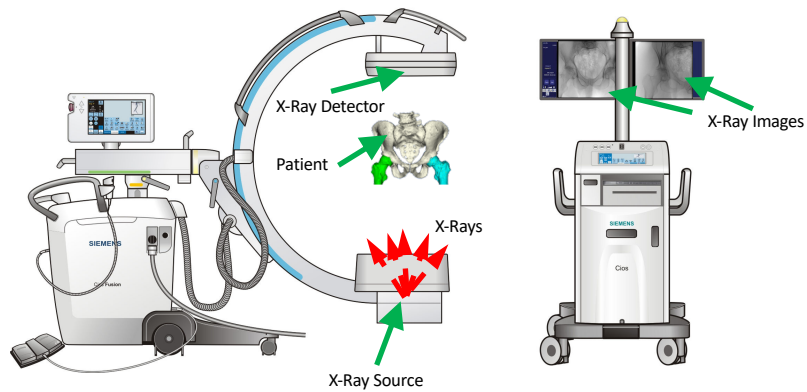
Copyright 2021 R. H. Taylor

Slide credit: Robert Grupp
Engineering Research Center for Computer Integrated Surgical Systems and Technology



89

Intraoperative X-Ray Imaging with Mobile C-Arm



C-Arm Image Source: Siemens CIOS Fusion Manual

Chapter 4: Pose Estimation Using Fluoroscopy

Copyright 2021 R. H. Taylor


Slide credit: Robert Grupp
Engineering Research Center for Computer Integrated Surgical Systems and Technology



90

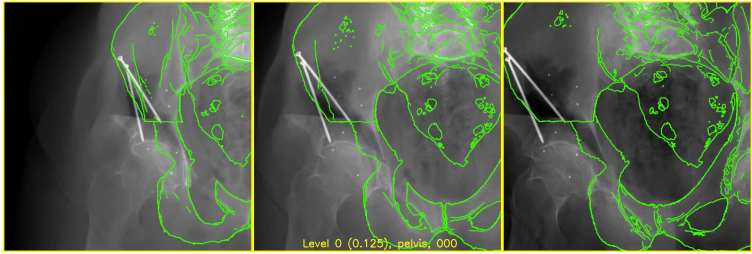
ciis

3D-2D Registration of Osteotomy Fragments

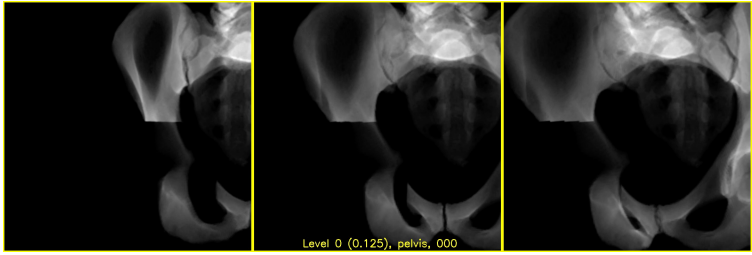


$$\arg \min_{\theta_1, \dots, \theta_N \in SE(3)} \sum_{m=1}^M \mathcal{S} \left(I_m, \sum_{n=1}^N \mathcal{P}_m(I_{CT}; \theta_n) \right)$$

Fixed Images
with Moving
Image Edges



Moving Images




R. Grupp, R. Murphy, M. Armand, R. Taylor

Copyright 2021 R. H. Taylor Slide credit: Robert Grupp Engineering Research Center for Computer Integrated Surgical Systems and Technology

91

ciis

3D-2D Registration of Osteotomy Fragments




- Compute the Sobel derivatives in the X and Y directions of the two input images:


$$\nabla_X I_1, \nabla_X I_2, \nabla_Y I_1, \nabla_Y I_2$$

- Compute NCC between the corresponding gradient images:


$$\mathcal{S}(I_1, I_2) = NCC(\nabla_X I_1, \nabla_X I_2) + NCC(\nabla_Y I_1, \nabla_Y I_2)$$



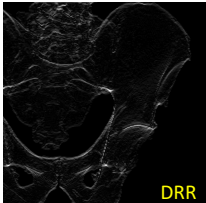
$\nabla_X I_1$



$\nabla_X I_2$



$\nabla_Y I_1$



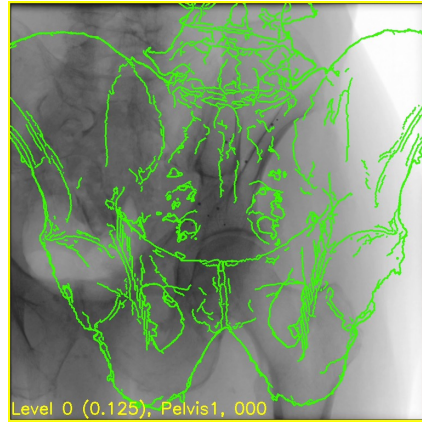
$\nabla_Y I_2$

R. Grupp, R. Murphy, M. Armand, R. Taylor

Copyright 2021 R. H. Taylor Slide credit: Robert Grupp Engineering Research Center for Computer Integrated Surgical Systems and Technology

92

Initialize Using a Nominal AP View?



Chapter 4: Pose Estimation Using Fluoroscopy

Copyright 2021 R. H. Taylor

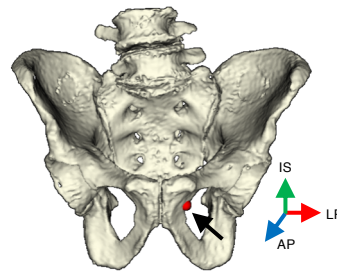
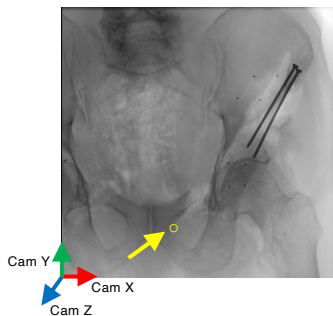
Slide credit: Robert Grupp
Engineering Research Center for Computer Integrated Surgical Systems and Technology



93

Use a Single Landmark to Initialize Registration

- Assume the pelvis is in an AP orientation – this may be computed preoperatively
- Manually annotate a single landmark to recover translation



Chapter 4: Pose Estimation Using Fluoroscopy

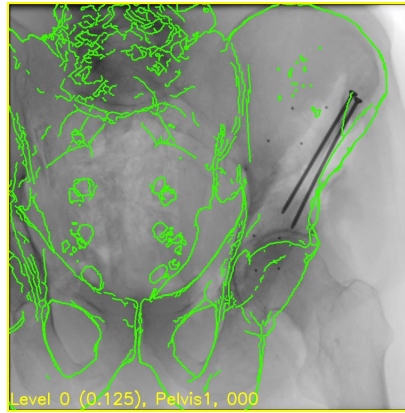
Copyright 2021 R. H. Taylor

Slide credit: Robert Grupp
Engineering Research Center for Computer Integrated Surgical Systems and Technology



94

Example of a Single Landmark Initialization



Chapter 4: Pose Estimation Using Fluoroscopy

Copyright 2021 R. H. Taylor

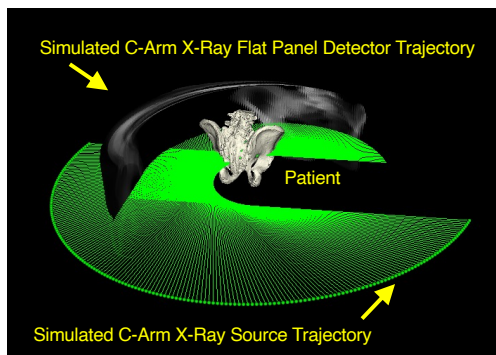
Slide credit: Robert Grupp
Engineering Research Center for Computer Integrated Surgical Systems and Technology



95

Automatically Initialize Second and Third Views

- Constrain C-arm motion to orbital rotation
- Perform an exhaustive search over $\pm 90^\circ$ in 1° increments



Chapter 4: Pose Estimation Using Fluoroscopy

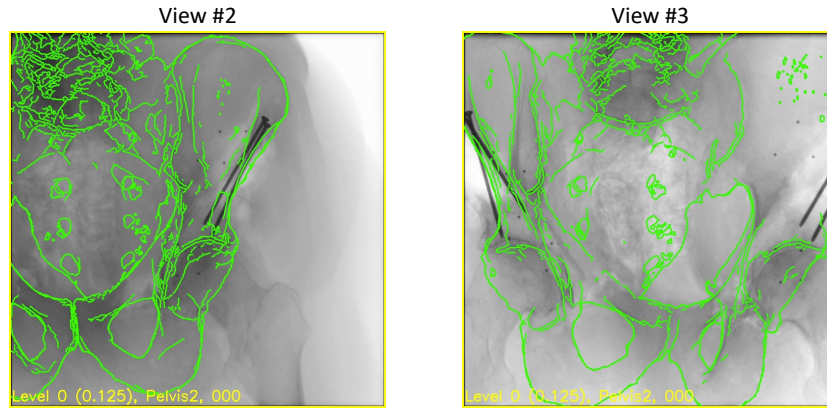
Copyright 2021 R. H. Taylor

Slide credit: Robert Grupp
Engineering Research Center for Computer Integrated Surgical Systems and Technology



96

Example Initializations From Orbital Search



Chapter 4: Pose Estimation Using Fluoroscopy

Copyright 2021 R. H. Taylor

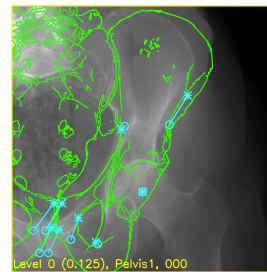
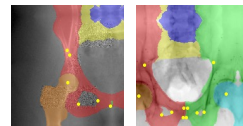
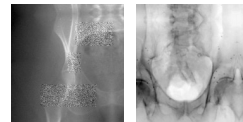
Slide credit: Robert Grupp
Engineering Research Center for Computer Integrated Surgical Systems and Technology



97

Automatic Landmark-Based Initialization

- Train a CNN to recognize approximate landmark positions in x-ray images
- Use landmark-based 2D-3D registration to initialize registration
- Combine landmark and intensity objective functions



Copyright 2021 R. H. Taylor

Images: Robert Grupp
Engineering Research Center for Computer Integrated Surgical Systems and Technology



98

Why Not Simultaneously Use Intensities and Features?

- Registration objective function:

$$\min_{\theta_P, \theta_{LF}, \theta_{RF} \in SE(3)} \lambda \mathcal{S}(\mathcal{P}(\theta_P, \theta_{LF}, \theta_{RF}), I) + (1 - \lambda) \mathcal{R}(\theta_P, \theta_{LF}, \theta_{RF})$$

↑ Image Similarity Term ↑ Regularization Term

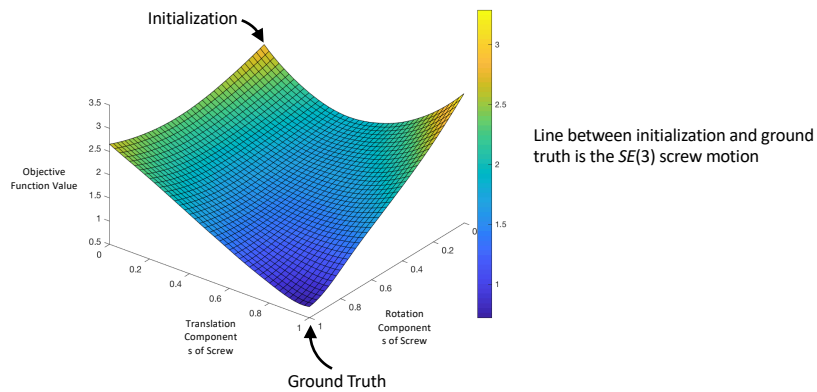
- Usually, regularization penalizes the amount of rotation and translation away from initialization
- Why not directly include the landmark re-projection as regularization?

$$\mathcal{R}(\theta_P) = \frac{1}{2\sigma_l^2} \sum_{l=1}^{N_l} \left\| \mathcal{P}(p_{3D}^{(l)}; \theta_P) - p_{2D}^{(l)} \right\|_2^2$$

- Can also think of this as running landmark registration and regularizing on image appearance

Chapter 6: Automatic and Robust Registration

Objective Function When Combining Landmark Re-Projection



Chapter 6: Automatic and Robust Registration